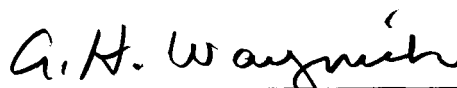Ionospheric Research

NASA Grant NsG-114-61

Scientific Report

on

Variations in the Total Electron Content of the Ionosphere

at Mid-Latitudes During Quiet Sun Conditions

by

Steven L. Solomon
November 30, 1965

Scientific Report No. 256

Ionosphere Research Laboratory

Submitted by: _W. J. Ross, Professor of Electrical Engineering_

Approved by: _A. H. Waynick, Professor of Electrical
Engineering, Director, Ionosphere Research
Laboratory_

The Pennsylvania State University

College of Engineering

Department of Electrical Engineering

TABLE OF CONTENTS

ABSTRACT   /5438

The Faraday rotation effect on satellite signals has been used to determine the electron content of the ionosphere at mid-latitudes. The ambiguity in the total number of rotations along the ray path has been resolved by using the method of closely-space frequencies.

Observations of the total electron content of the ionosphere made over a five month period are presented and compared with values obtained in similar experiments in previous years. Horizontal gradients are discussed with sunrise effects being considered. Diurnal and day-to-day variations in content are shown, and conclusions are drawn associating variations in the magnitude and gradient of the total electron content with magnetic activity.

Author

I. INTRODUCTION

1. The Ionosphere[20]

The ionosphere is a region of the atmosphere, extending from about 60 km upwards in altitude, in which the constituent gases are partially ionized.

The production of free electrons and positive ions in the atmosphere is due to photoionization by ultraviolet and X-radiation from the sun. As the radiation penetrates deeper into the atmosphere, the production rate per unit volume increases because the gaseous density in increasing; however, the radiation is absorbed in the production process and a level is reached below which the production rate decreases. The principal loss process for free electrons in dissociative recombination which is the recombination of a free electron and an ionized molecule with subsequent dissociation of the molecule.

2. Methods of Studying the Ionosphere

The most widely used method of studying the height distribution of free electrons in the ionosphere has been the pulse sounding method. This consists of sending radio frequency pulses vertically from the ground into the ionosphere and measuring the delay time for an echo to return. Delay time is measured as a function of frequency by an instrument known as an ionosonde, and the resulting records are known as ionograms. The recording of ionograms has taken place for many years at stations throughout the world; methods have been developed to deduce electron density as a function of

height from these records. They have been used to obtain the electron density height profile up to the electron density maximum, N_{max}. The frequency at this point is critical, and above it the radio waves penetrate the ionosphere and do not return to the earth. Measurements of this nature have led to a general description of the bottomside ionosphere.

Techniques have been developed to study the total ionosphere. Measurements above N_{max} have been made using rockets, artificial satellites, incoherent scattering of radio waves by free electrons, radio star emissions, and radio echoes from the moon. Since 1962, the "Alouette" topside sounder satellite has been used for radio wave probing above N_{max} and has yielded a large number of electron density-height profiles.

3. Satellite Beacon Experiments

The placing of the first artificial earth satellite in orbit by the USSR marked the beginning of new scientific experiments making use of satellites as a new experimental tool. This satellite allowed the measurement of propagation effects over the transmission path from the satellite to earth.

Satellite experiments based on both polarization rotation and phase path dispersion measurements have made available data of the total electron content of the ionosphere, since if the satellite entire ionosphere can be studied. The satellite orbit generally precesses so that the time of observation by a particular ground

station is different each day. Over a number of weeks the satellite pass time precesses through twenty-four hours, making observations of diurnal variations in electron content possible. Seasonal variations in electron content can also be observed, provided the active life of the satellite is sufficiently long.

A disadvantage in satellite total electron content measurements is that there is no way of determining the distribution of electrons between the satellite and the observer.

4. Statement of the Problem

The S-66 Ionosphere Beacon Satellite was specifically designed for ionosphere research by means of radio transmissions. It was launched on October 10, 1964 by the National Aeronautics and Space Administration. Signals are recorded whenever the satellite is in the field of view of the receiving station at University Park, Pennsylvania (40.8°N, 77.9°W).

It is proposed that the method of Faraday rotation be used to calculate the total columnar electron content between the station and the path of the satellite using the 40 MHz and 41 MHz signals from the S-66 satellite. Although total electron content is not an ionospheric parameter that has been widely used in the past, it is very useful in interpreting other ionospheric data, it serves as a check on the determinations of the electron density profile, and it is readily correlated with other geophysical phenomena.

It is further proposed to compare the total electron content with results obtained from similar experiments in previous years.

The horizontal gradient of the content will be examined and variations in both the magnitude and the gradient of the electron content will be analyzed. An attempt will be made to associate these variations with magnetic activity.

II. THEORY

1. First-order Theory of Faraday Rotation

A linearly polarized radio wave traveling through a homogeneous ionized medium, such as the ionosphere, is equivalent to two components, the ordinary and extraordinary waves of the magneto-ionic theory, which are generally elliptically polarized with opposite senses of rotation and which travel with different velocities. For a sufficiently high frequency (wave frequency >> collision, plasma, and gyromagnetic frequencies) and a direction of propagation which is not too nearly normal to the magnetic field, these waves will be nearly circularly polarized. They also have complex, anisotropic, refractive indices, i.e. they are absorbed as they propagate, and for neither characteristic wave do the wave-normal and ray directions coincide. Since the refractive indices are different, i.e., the two components have different phase velocities, the plane of polarization of the resultant wave field gradually rotates as the wave progresses through the ionosphere. This phenomenon is known as the ionospheric Faraday effect.

An expression for the total number of rotations of the plane of polarization of the resultant wave will be derived. Since the instantaneous electric vector for each component rotates through 2π radians for each wavelength of phase path, their incremental rotations are given by

$$d\phi_o = 2\pi \frac{ds}{\lambda_o} \quad \text{and} \quad d\phi_e = 2\pi \frac{ds}{\lambda_e}$$

where $d\phi_o$ = rotation of the ordinary wave

$d\phi_e$ = rotation of the extraordinary wave

ds   = an increment of path length

λ_o = wavelength corresponding to ordinary phase velocity

λ_e = wavelength corresponding to extraordinary phase velocity

Figure 1 shows the relation between $d\phi_o$, $d\phi_e$, and $d\Omega$, the number of rotations (one rotation = π radians) through which the plane of polarization rotates as the wave travels the distance ds. From this figure

$$d\phi_e + (d\Omega)\, \pi \;=\; d\phi_o - (d\Omega)\, \pi$$

or

$$d\Omega \;=\; \frac{d\phi_o - d\phi_e}{2\pi} \qquad .$$

Substituting for $d\phi_o$ and $d\phi_e$ yields

$$d\Omega \;=\; \frac{2\pi ds/\lambda_o - 2\pi ds/\lambda_e}{2\pi} \;=\; \left(\frac{1}{\lambda_o} - \frac{1}{\lambda_e} \right) ds \quad .$$

Using the relations $\lambda = v/f$ and $v = c/n$, λ can be expressed in terms of index of refraction n, frequency f, and free space velocity c; this gives the expression

$$d\Omega \;=\; \frac{f}{c}\,(n_o - n_e)\,ds \quad . \tag{1}$$

Appleton and Hartree[19] have shown that the expression for the index of refraction of an ionized medium with a magnetic
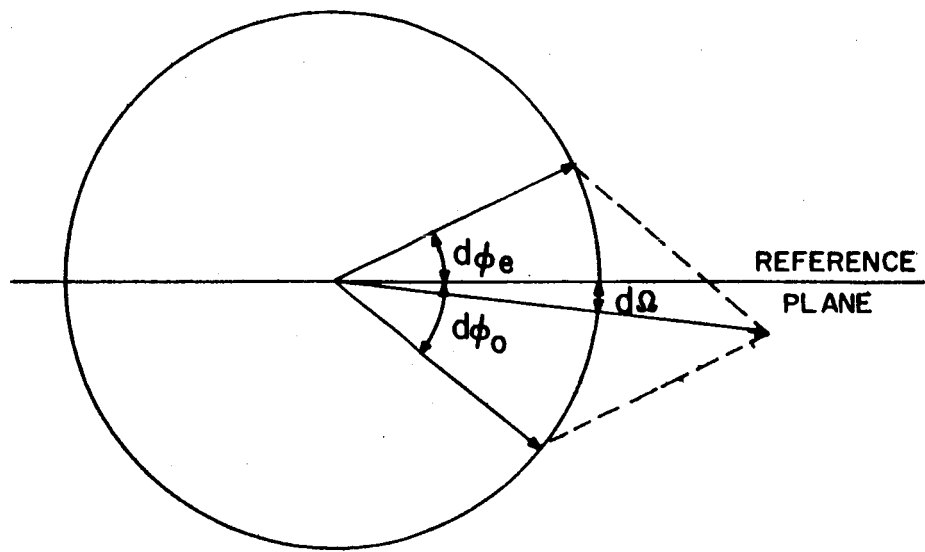
RELATIONSHIP BETWEEN $d\phi_o, d\phi_e$ AND $d\Omega$

FIGURE I

field is

$$n_{o,e}^2 = 1 - \cfrac{X}{1 - iZ - \cfrac{Y_T^2}{2(1-X-iZ)} \pm \left[\cfrac{Y_T^4}{4(1-X-iZ)^2} + Y_L^2\right]^{\frac{1}{2}}}$$

where $X = f_N^2/f^2$

$Y_L = f_L/f$

$Y_T = f_T/f$

$Z = \nu/2\pi f$

$f_N^2 = Ne^2/4\pi^2 \epsilon_o m$

$f_L = (Be/2\pi m) \cos \theta$

$f_T = (Be/2\pi m) \sin \theta$

f = wave frequency

ν = frequency of collision of electrons with heavy

particles

N = number density of electrons

e = the charge of an electron

m = mass of an electron

ϵ_o = electric permittivity of free space

B = induction of the imposed magnetic field

θ = the angle between the magnetic field and

the wave normal

All quantities are in rationalized MKS units.

For a wave frequency of 40 MHz which is much greater than the collision frequency, the difference between the absorption indices of the two modes is much less than one so the previous equation can be reduced to

$$n_{o,e}^2 = 1 - \frac{X}{1 - \frac{Y_T^2}{2(1-X)} \pm \left[\frac{Y_T^4}{4(1-X)^2} + Y_L^2 \right]^{\frac{1}{2}}} .$$

Use will now be made of the QL (quasi-longitudinal) approximation. The condition for this is that

$$\frac{Y_T^4}{4Y_L^2} \ll |1 - X|^2 .$$

Rewriting in terms of frequency

$$\left| \frac{Be}{2m} \sin \theta \tan \theta \right|^2 \ll \left(2\pi \frac{(f^2 - f_N^2)}{f} \right)^2 .$$

The QL inequality is at least 1:10 for a wave frequency of 40 MHz provided θ is not between 87° and 93°. In other words, except for rays that are within three degrees of being perpendicular to the geomagnetic field, the propagation is quasi-longitudinal. This means that the index of refraction assumes the form

$$n_{o,e} = \left(1 - \frac{X}{1 \pm |Y_L|} \right)^{\frac{1}{2}} .$$

At 40 MHz both $X \ll 1$ and $|Y_L| \ll 1$ so that $n_{o,e}$ may be

written approximately

$$n_{o,e} = 1 - \frac{X}{2} (1 \mp |Y_L|)$$

Thus

$$n_o - n_e = 1 - \frac{X}{2} (1 - |Y_L|) - (1 - \frac{X}{2} (1 + |Y_L|) = X|Y_L|$$

Substituting this expression into equation (1)

$$d\Omega = \frac{f}{c} (XY_L) ds = \frac{f}{c} \left(\frac{f_N^2}{f^2} \frac{f_L}{f} \right) ds = \frac{f}{c} \left(\frac{Ne^2 Be \cos\theta}{4\pi^2 \epsilon_o m f^2 2\pi m f} \right) ds$$

$$= \frac{Ne^2 B \cos\theta}{8\pi^3 cm^2 \epsilon_o f^2} ds = \frac{e^3}{8\pi^3 c\epsilon_o m^2} \frac{B \cos\theta N ds}{f^2}$$

If we wish to find the total number of rotations of the plane of polarization, assuming that the two modes follow a common path P, we integrate to find

$$\Omega = \frac{e^3}{8\pi^3 c\epsilon_o m^2} \frac{\int_P B \cos\theta N ds}{f^2} = 7.53 \times 10^3 \frac{\int_P B \cos\theta N ds}{f^2}$$

If it is assumed that the ionosphere does not vary horizontally and that the ray is straight, it can be written that

$$ds = dh \sec\chi \quad ,$$

where dh is an element of height and χ is the angle between the ray and the vertical. Then Ω becomes

$$\Omega = \frac{7.53 \times 10^3}{f^2} \int_0^{h_s} NB \cos\theta \sec\chi \, dh ,$$

where h_s is the upper extreme of one end of the path. Enough is known about the electron distribution so that the mean ionosphere height is determined reasonably accurately. Since $B \cos\theta \sec\chi$ is slowly varying, its value calculated at this height can replace the expression in the integral. The equation then becomes

$$\Omega = \frac{7.53 \times 10^3}{f^2} \overline{B \cos\theta \sec\chi} \int_0^{h_s} N \, dh . \qquad (2)$$

Thus the plane of polarization of the wave undergoes a rotation which is directly proportional to the integrated electron content.

Since the initial polarization is not known and the plane of polarization is unaltered by the addition to Ω of $n\pi$ ($n = 0, 1, 2, \ldots$), the total angle of rotation cannot be found unambiguously using a single frequency at mid-latitudes. In order that this total angle be unambiguously determined, use may be made of the relation $\Omega \propto 1/f^2$. This technique involves the observation of slow fading on two closely-spaced frequencies.

If there is a difference of $\Delta\Omega$ in the amounts of rotations of the two frequencies which are separated by a small amount Δf, then Ω can be found in terms of $\Delta\Omega$.

$$\Omega' - \Omega = \Delta\Omega$$

where the primes will denote the second frequency so that

$$\frac{\Delta\Omega}{\Omega} = \frac{\Omega'}{\Omega} - 1 = \frac{f^2}{f'^2} - 1 = \frac{f^2 - f'^2}{f'^2} \quad . \tag{3}$$

2. Application to Satellite Observations[2, 9, 13]

For the determination of integrated electron content, transmissions from the S-66 satellite are being used. The satellite is in a near-polar orbit well above the F region of the ionosphere. Maximum Faraday rotation will be obtained for propagation directions that are not too nearly perpendicular to the earth's magnetic field and for frequencies that are low (because of $1/f^2$ dependence) but sufficiently above the plasma frequency of the F layer. For this latter reason, frequencies of 40 MHz and 41 MHz are transmitted from the beacon satellite.

When the satellite is to the south, the rotation angle is relatively large since both $\cos\theta$ and $\sec\chi$ are large. When the satellite is at the point of closest approach, the rotation angle is found to be smaller, owing largely to the reduction in $\sec\chi$. As the satellite continues its travel to the north, the rotation angle still continues to decrease because the reduction of $\cos\theta$ more than offsets the increase in $\sec\chi$. If the ray path could become transverse to the magnetic field, the total rotation angle would be reduced to a small fraction of the overhead value which to a first approximation may be equated to zero. The locus of points where this

theoretically takes place is below the radio horizon, and from one of these points we have effectively counted the number of Faraday rotations of the received signal as the satellite moves through this point to any point on the trajectory. From this number of rotations the electron content of that part of the ionosphere between observer and satellite is calculated for various points along the trajectory and hence the variation of the electron content along a slice of the ionosphere can be determined.

Going back to equation (2), if 41 MHz is inserted for the wave frequency the expression becomes

$$\Omega = 4.48 \times 10^{-12} \; \overline{B \cos \theta \sec \chi} \int_{0}^{h_s} N \, dh \; .$$

In terms of electron content, this can be written as

$$\int_{0}^{h_s} N \, dh = 2.23 \times 10^{11} \; \frac{\Omega}{\overline{B \cos \theta \sec \chi}} \tag{4}$$

Now use must be made of equation (3) to get Ω in terms of $\Delta\Omega$. Letting the prime terms refer to 40 MHz and the unprimed terms to the 41 MHz signal, $\Omega = 19.75 \; \Delta\Omega$.

3. Second-Order Theory[22]

The Faraday effect equations have been extended to include second-order effects. First-order theory is based on straight line propagation and second-order theory concerns the following departures from this:

(1) The non-uniform distribution of ionization causes the various rays to be refracted and follow different paths between source and receiver.

(2) Since the medium is anisotropic, the wave normal and ray for a particular mode of propagation are not coincident in direction.

(3) The refractive index is non-linear in electric density and magnetic field intensity.

The second-order polarization rotation angle was derived as

$$\Omega_2 = \Omega\left[1 + \frac{\beta\overline{X}}{2} + \frac{(\beta-1)}{2}\ G\overline{X}\ \right]$$

where

Ω_2 = second-order polarization rotation angle

Ω = first-order polarization rotation angle as previously defined

$$\overline{X} = \frac{e^2}{\epsilon_o m 4\pi^2 f^2}\ \frac{\int_o^{h_s} N\,dh}{h'} = \frac{4.91 \times 10^{-14}\int_o^{h_s} N\,dh}{h'}$$

$h' = h_s + R_o(1 - \cos C2)$

R_o = radius of the earth

$C2$ = central angle between station and satellite

$\beta = \dfrac{\overline{X^2}}{\overline{X}^2}$ = a measure of the non-uniformity of the ionization distribution over the height of integration to the satellite

G = a geometrical parameter involving the direction

of straight line propagation, the magnetic field,

and the vertical at the ionosphere point near which

the bulk of ionization lies

When applying the theory to close-spaced frequency polarization rotation dispersion, the second-order correction is found to be twice as great as that for the polarization rotation itself, for

$$d\Omega_2 = -2\Omega \frac{df}{f} [1 + \beta\overline{X} + (\beta-1) G\overline{X}]$$

instead of $d\Omega = -2\Omega df/f$ as in first-order theory. The measured value of Ω must then be adjusted to a corrected value which is done by multiplying it by $(1 - \beta\overline{X} - (\beta-1) G\overline{X})$. This new value of Ω is then used in the first-order equations previously derived.

III. INSTRUMENTATION

1. Satellite

The S-66 Ionospheric Beacon Satellite provides a means for obtaining Faraday rotation and differential Doppler ionospheric measurements on all parts of the globe over an extended period of time.

The orbit is almost polar and circular to obtain worldwide coverage and simplify interpretation of the measurements, respectively. The satellite beacon is nominally at 1000 Km altitude so that it is above the major portion of the ionosphere's electron content.

Initial orbit properties were:

Anomalistic period	104.76 minutes
Inclination	79.61 degrees
Perigee	880 Km
Apogee	1080 Km

There are four transmitters operating continuously at 20 MHz, 40 MHz, 41 MHz and 360 MHz; the first three have a nominal power of 250 mw while the 360 MHz signal has a radiated power of 100 mw.

The satellite radiates linear polarization from dipoles normal to its axis. The axis is magnetically oriented along the local magnetic field at the orbit height; therefore, at mid-latitudes it is seen from one end only. The spin about the axis is damped mechanically to a rate designed to be less than 0.02 rotations per minute.

The satellite period and the precession of the orbit plane
are such that almost fourteen complete orbits occur in one day. If
the first orbit is directly over the receiving station, the fifteenth
will pass approximately one day and twenty-seven minutes later and
8.94 degrees further west in longitude. Consecutive orbits cross
the station latitude separated by 104.76 minutes in time and 26.35^{o}
in longitude. Only satellite passes which cross the receiving station
latitude within 25 degrees east or west of the receiving station
longitude are recorded. Therefore, the precession of satellite
pass time is such that observations are made twenty-seven minutes
later each day for two days; on the third day another satellite pass
is observed seventy-eight minutes earlier. Thus, the overall trend
of time of satellite passes is backward through time of day, an
average of eight minutes per day. During a six month period, the
time of a satellite pass precesses backward through twenty-four
hours.

Usually two consecutive north-going passes were observed,
and eleven hours later two consecutive south-going passes each day.

2. Receiving and Analysis Equipment

The block diagram of the receiving and analysis equipment
is shown in Figure 2. Used for Faraday rotation are the 20 MHz,
40 MHz, and 41 MHz signals received on fixed linearly polarized
dipole antennas and recorded on magnetic tape, together with the
standard time. When the tapes are played back, the signals are
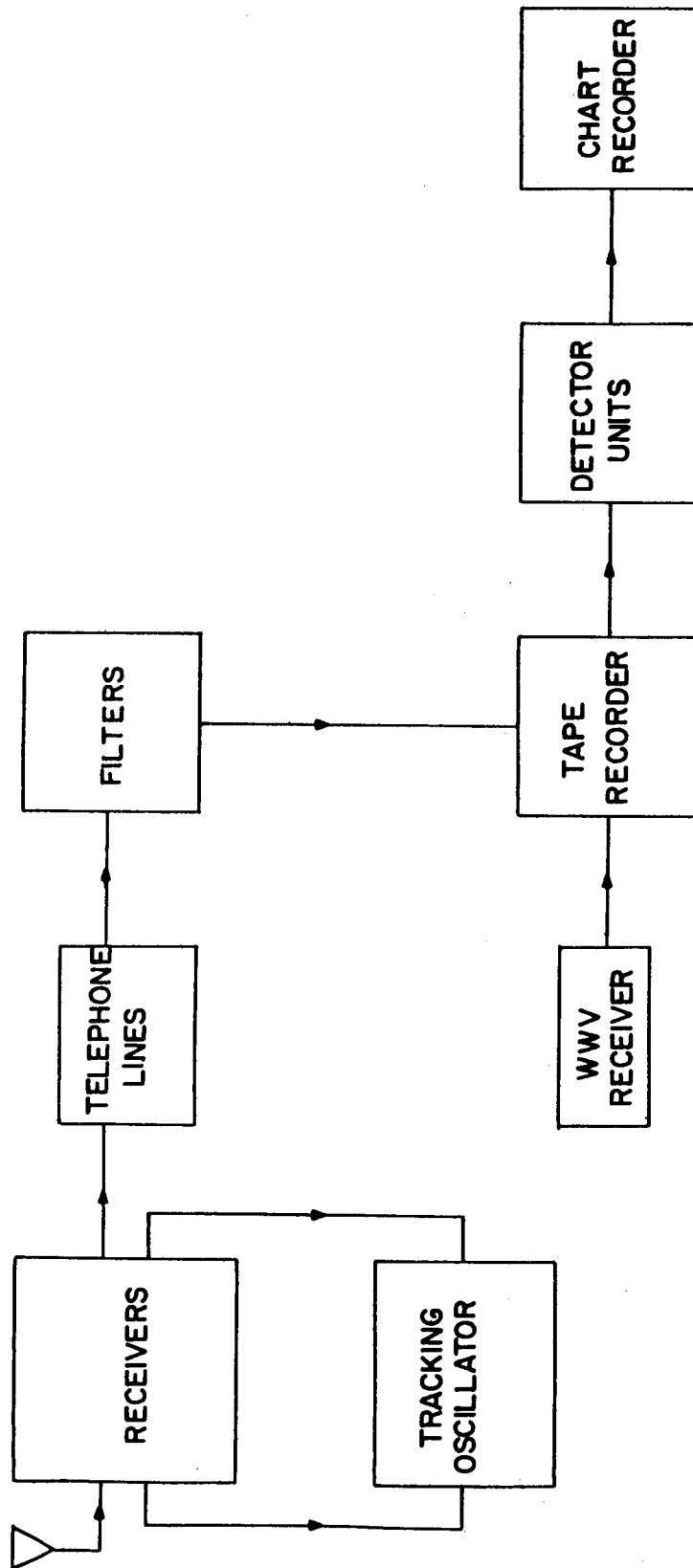
BLOCK DIAGRAM OF FARADAY RECEIVING AND ANALYSIS EQUIPMENT

FIGURE 2

filtered and envelope detected and recorded on a multichannel

Sanborn chart recorder as shown in Figure 3.
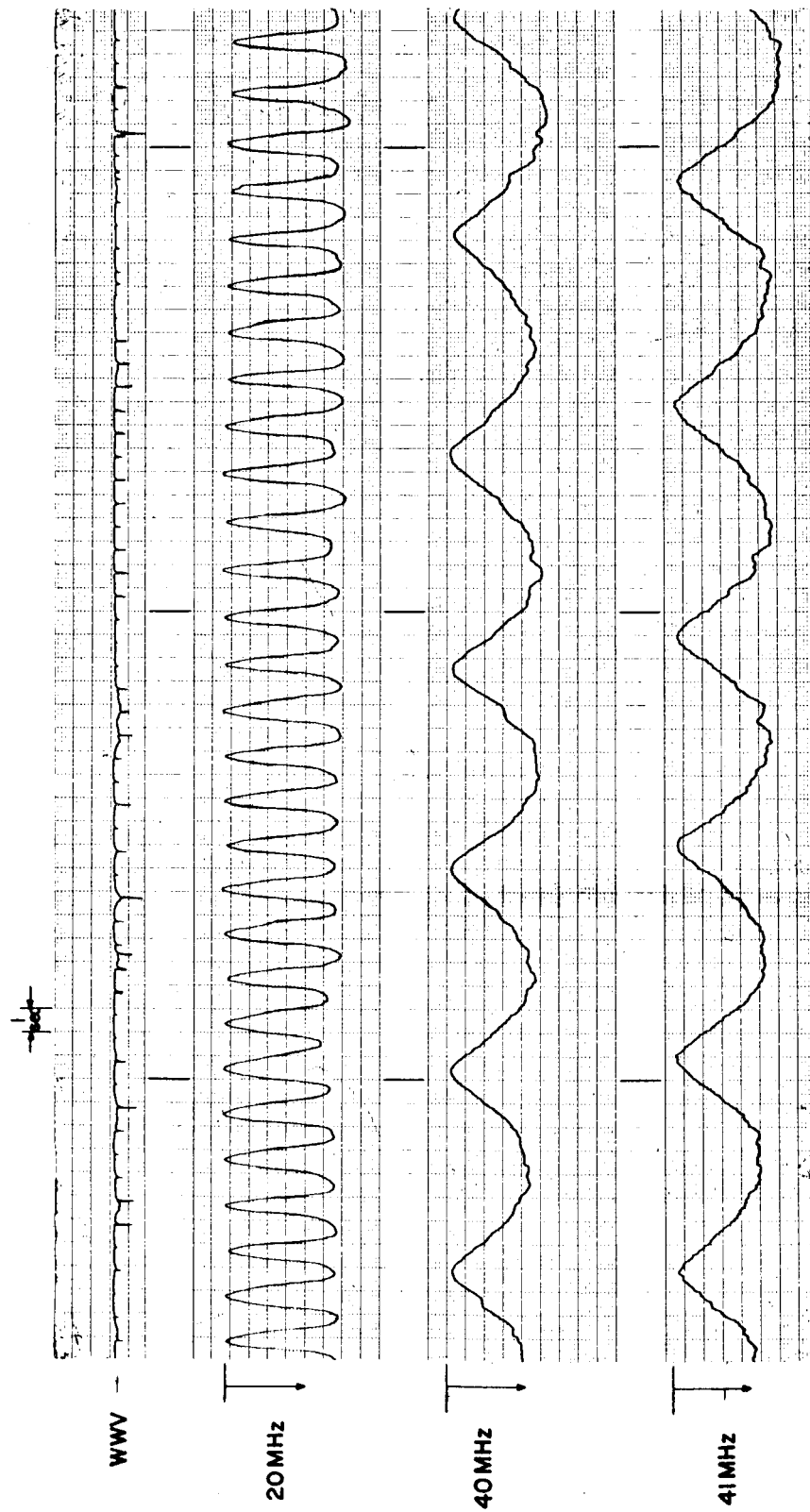
SAMPLE RECORDING OF SATELLITE SIGNALS

FIGURE 3

IV. METHOD OF ANALYSIS

1. Counting of Rotations

The sample recording of part of a pass in Figure 3 contains the WWV trace showing the Eastern Standard Time every second. The reading accuracy is limited by the sharpness of the nulls of the 40 MHz and 41 MHz signals whose times must be read.

Each successive null to the south represents one more rotation of the plane of polarization of the propagated signal since the satellite passed through the theoretical transverse point which is below the radio horizon to the north; it is not known how many rotations have been made before the northernmost null recorded. Use must be made of the previously stated relationship

$$\Omega = 19.75 \, \Delta\Omega$$

to solve this problem which is now reduced to finding the fractional difference of rotation between the 40 MHz and 41 MHz nulls. This can be done by linear interpolation to the 41 MHz null, assuming a constant rate of rotation between the adjacent 40 MHz nulls. The procedure has been simplified by using an expanding scale and reading the fraction directly.

In many cases the assumption of a linear rate of rotation between adjacent pairs of nulls proved to be erroneous and yielded misleading results; this necessitated altering the method of counting the rotations. By observing the 20 MHz nulls, it is possible to determine where, in fact, the 40 MHz rotation is essentially linear.

For each pass then, a pair of 40 MHz nulls is carefully chosen with regard to the aforementioned linearity. The fractional and then the total rotation is calculated for the bracketed 41 MHz null. For each 41 MHz null to the south of this null, one rotation is added successively; for each to the north, one is subtracted successively. The time is read at each 41 MHz null, thus giving a time and a value of Ω for each null.

2. Resolution of Ambiguities

Unlike fractional differences, an integral difference of rotation cannot be measured directly. In other words, there is ambiguity involved as to whether to any measured fractional difference on integer should be added.

Several methods are used to resolve this ambiguity. First of all, the chosen null is picked as far to the north as possible, still observing the linearity previously discussed; the fractional rotation is generally less than unity a reasonable distance north of the station. Also by looking at the entire trace, it can sometimes be determined whether the fractional rotation is greater than one, since $\Delta\Omega$ must always be greater than zero. Lastly, the results can be compared for the different possibilities, and generally only one will give reasonable results for electron content, especially with regard to magnitude, gradient, and time of day. All of these checks will combine to resolve the ambiguity in virtually all instances.

Another problem which arises is the detection of a reversal of the sense of rotation. This takes place rarely and briefly and

only when there is a comparatively large variation in ionization over a small interval. Thus for a southgoing pass, a sudden decrease in electron content may cause the plane of polarization to stop and reverse its direction for a short while. From the 41 MHz signal alone there is no sure way to determine when this happens. Usually a reversal can be recognized when there is a change in the pattern of the two sets of nulls at 40 MHz and 41 MHz. The 20 MHz nulls are then used to determine when the rotation reversed and then where it returned to its original sense. This is possible to do since there is a constant ratio of nulls from the 20 MHz signal to the others of approximately four-to-one. Subsequent nulls must then be adjusted to their proper numerical value.

3. Calculation of Results

It has been shown that the observed data yield the number of polarization rotations at different times. The orbital data supplied by NASA give the latitude, longitude, and height of the satellite every minute, and since the satellite travels at approximately constant speed, linear interpolation is used to find the location at the time of each null.

The next step is to find $\overline{B \cos \theta \sec \chi}$ at each of these locations. This is also done with sufficient accuracy by linear interpolation of values which have been pre-computed at integral latitudes in satellite position from 22N-60N, integral longitudes from 50W-103W, and 100 Km intervals of satellite height. The values of G are found in a similar manner by interpolation of a

pre-computed grid.

At this point, the first-order value of $\int N\,dh$ is found using equation (4). An ellipsoidal earth is assumed in converting satellite position to ionosphere position at the mean ionosphere height that has been used.

It is then a simple matter to calculate $\overline{X}$ and then with values of G and β (which is assumed to be 2.5 based on electron density profiles) determine the second-order electron content for a meter square column extending vertically from the earth through the ionosphere up to the satellite height.

Most of the calculations were done on the IBM 7074 digital computer at The Pennsylvania State University.

4. Errors

The second-order theory has eliminated most of the systematic errors encountered when making simplifying approximations. In the extreme northern part of the pass, the second order content will be as much as 5% higher than first order. This difference gradually diminishes and becomes zero slightly north of the station at about $43^\circ N$. Further south, the second order content gradually becomes lower than the first order value, with as much as a 5% difference at the extreme southern end.

As stated before, much care was taken in determining where to calculate the fractional difference of rotation. For the most part, any error incurred here will virtually disappear except in the northern end of the pass where the number of rotations are very

small. Even then, this error will be substantial only when there is non-linearity between the 20 MHz nulls which enclose the chosen 41 MHz null, or if this null cannot be read accurately. By choosing a point in the north instead of the south to determine the rotation, the percent error would remain the same, but the actual number of rotations in error would be significantly less. This actual rotation is the important thing since the rotations at all other nulls would contain the same error. Nevertheless, a one-tenth second difference in the time of the null can result in as much as a 1% error in $\Delta\Omega$ during the day. For this reason, a null which cannot be read this closely should not be considered then. The allowable tolerance will increase with the time between nulls.

An error could be caused by rotation of the plane of polarization due to the spinning of the satellite about its magnetic axis; however, in the original specifications published, the satellite is said to spin less than 0.02 revolutions every minute, which is negligible compared with the measured polarization rotation rates.

Another source of error is in the scaling process; i.e. the reading of the times of the observed nulls. Most nulls are of sufficient sharpness to be read to the nearest tenth of a second; however, there are a few others in which the uncertainty is as much as a full second, most of these being at night when the rotation rate is slow. A time displacement of one second will result in a distance displacement of less than 0.06° latitude for the satellite with the longitude and height displacements being negligible. This will result in a change of less than 0.25% in $\overline{B \cos \theta \sec \chi}$ which is very small

considering the accuracy of this term.

In the calculations the mean ionosphere height was assumed to be 250 km based on a study of electron density profiles. A height of 300 km would have been closer to the true value at night but the daytime results will be of more use for this report, so the lower value was chosen. A comparison in the results using the two heights is shown in Figure 4. The difference in the content calculations is greater as the satellite is further to the north of the station. Also, being further to the west will increase the difference to as much as 15%. It should be noted that the content calculation for a particular null will be for different meter square columns in the ionosphere for each of the heights. The effect of both of these differences is best shown in the curves.

(In this and all other plots of electron content versus latitude the six digit number at the end of each curve will signify the date. The first two digits represent the year; the second two, the month; and the last two, the day. The four digit number is the approximate Eastern Standard Time the satellite was travelling across the station latitude.)
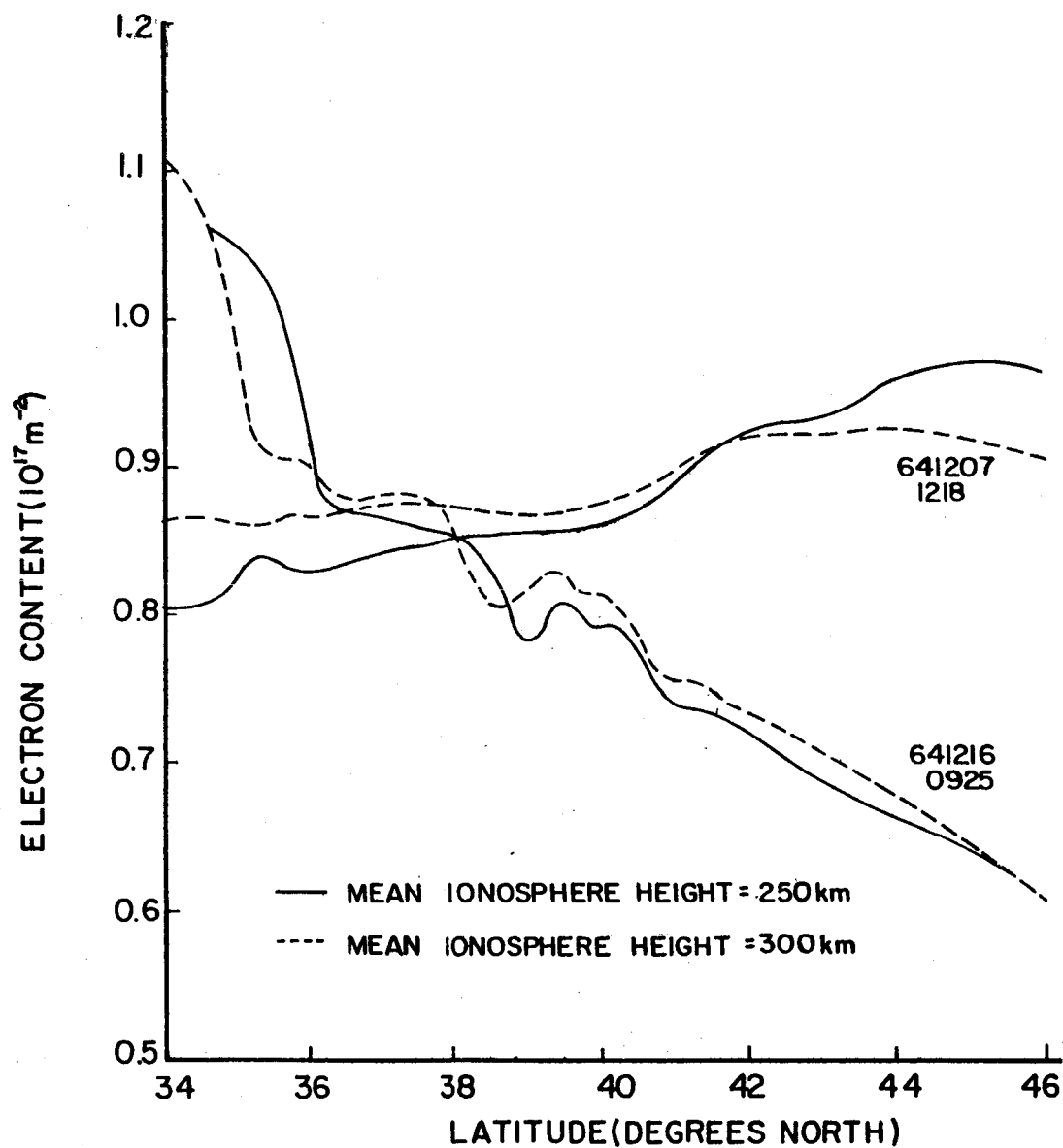
ELECTRON CONTENT vs. LATITUDE FOR
DIFFERENT MEAN IONOSPHERE HEIGHTS

FIGURE 4

V. RESULTS

Total electron content has been calculated for 285 passes of
the S-66 satellite observed at University Park, Pennsylvania
(40. 8°N, 77. 9°W) between October 24, 1964 and March 16, 1965.
During this five month span both the northgoing and southgoing
passes precessed 20 hours thus yielding results during two different
months for most periods of the day or night.

An analysis of these results with regard to magnitudes,
gradients, and variations of the electron content is found in
subsequent sections. An overhead value of the electron content of
the ionosphere has been determined from each pass and will be
found in the Appendix.

The observed daily values of the solar flux at 2800 MHz,
S, varied from 69. 9 to 85. 6 x 10^{-22} watts/m^2/Hz. The magnitude
of S is an indication of the intensity of the solar radiation which is
a source of electron production. These values of S are relatively
small so that the total electron content is expected to be small
compared to what it is during a period of high solar activity.
Furthermore, the changes in S were always less than 5% from one
day to the next.

1. Diurnal Variation

The total electron content for southgoing and northgoing
passes has been plotted in Figure 5A and 5B respectively with
local time as the abscissae. The content at 41°N was chosen,
regardless of any horizontal gradient. The midday period for the
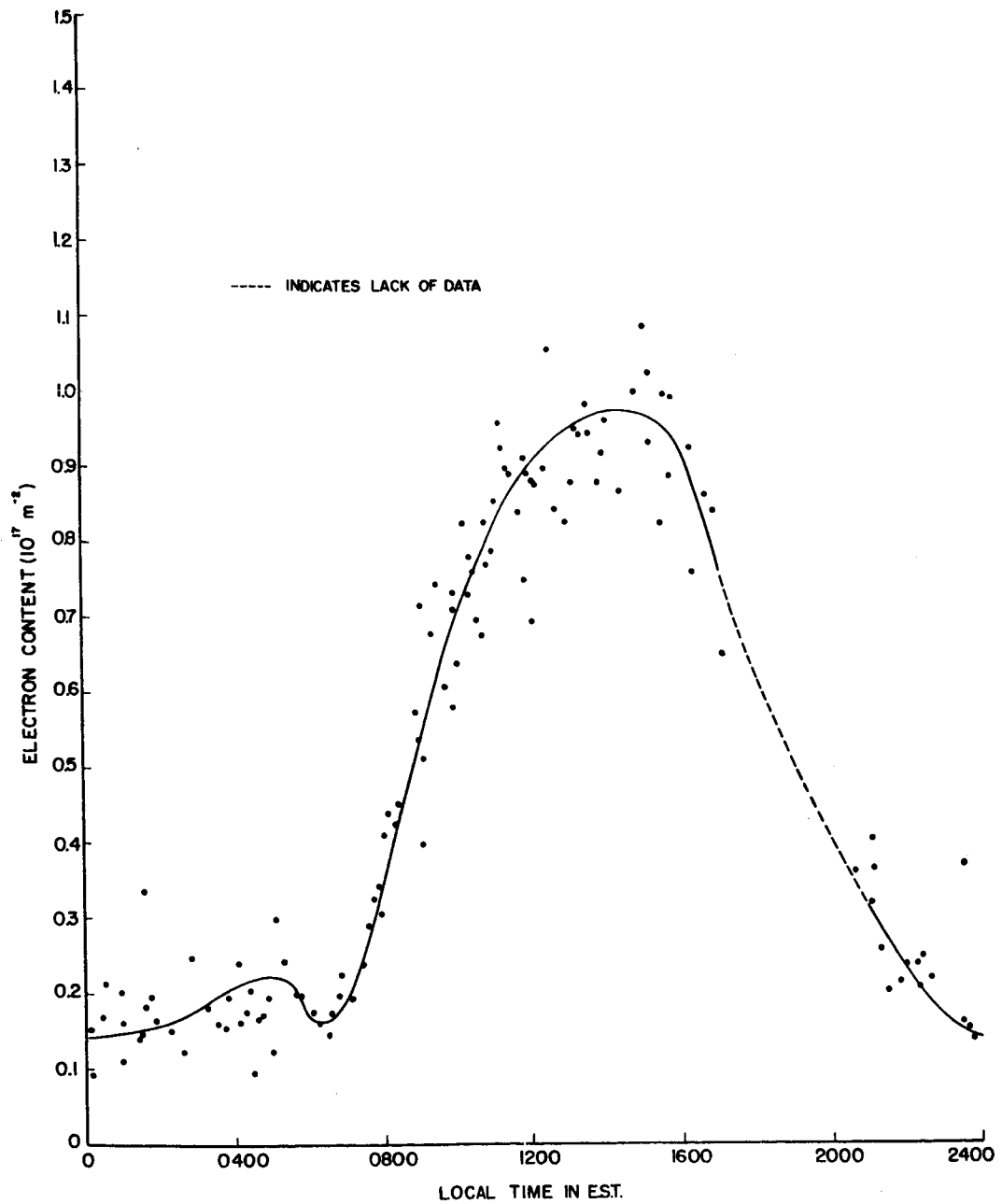
DIURNAL VARIATION OF ELECTRON CONTENT FROM
SOUTHGOING SATELLITE PASSES

FIGURE 5A
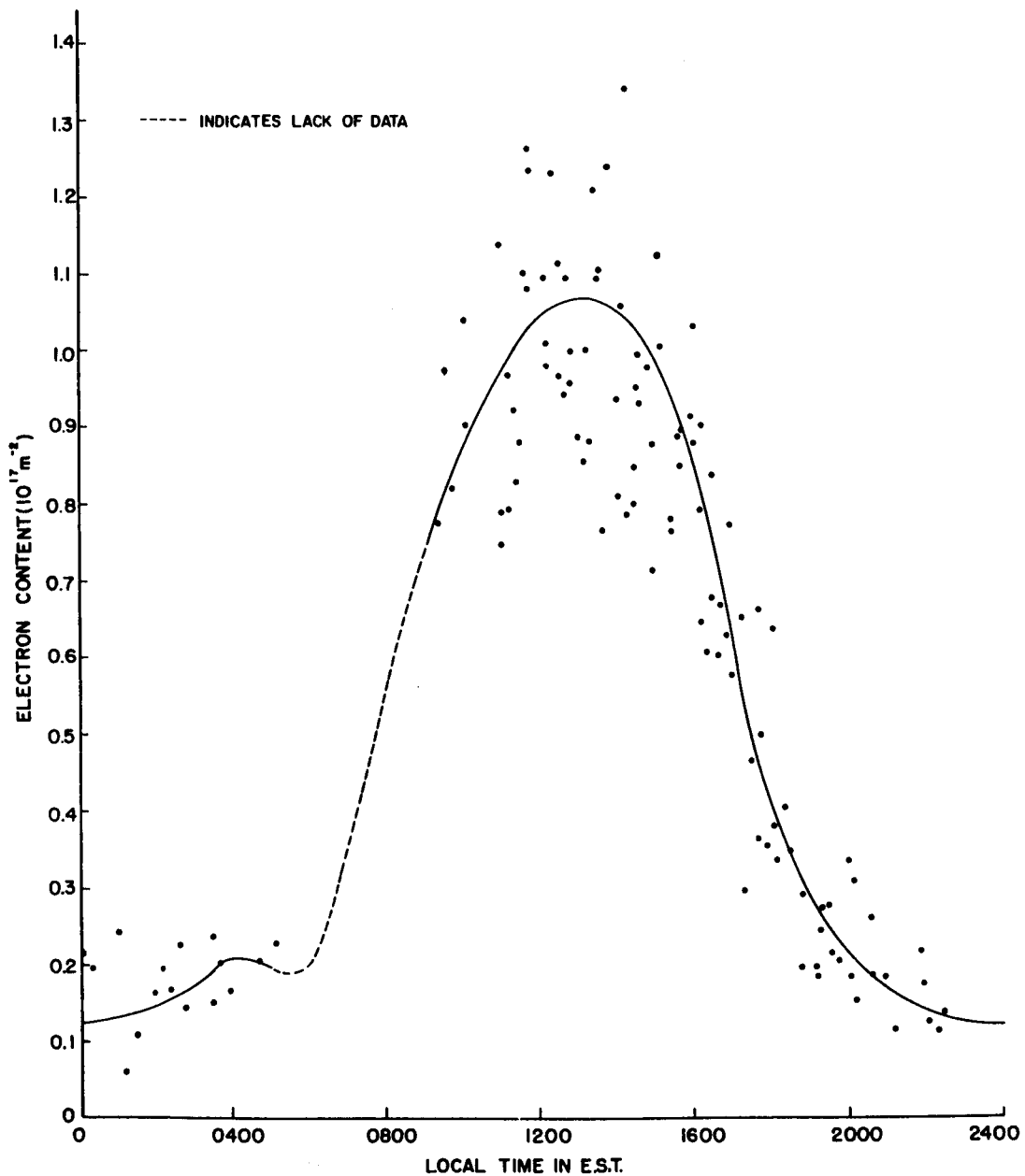
DIURNAL VARIATION OF ELECTRON CONTENT FROM
NORTHGOING SATELLITE PASSES

FIGURE 5B

southgoing passes was in November, 1964, while that for the north-
going was in February, 1965.

As expected there seems to be a steady average increase in
total electron content from about sunrise through the day to mid-
afternoon. Also the ratio of daytime maximum to nighttime
minimum is between 5 and 10 to 1 which confirms previous results.
(14, 16) The maximum values of the electron content seem to occur
a little later in the day in November than in February.

In Table 1 these results are compared to those of other
years extending from the last sunspot maximum. The solar index S
is tabulated as a measure of solar activity. It is apparent from the
table that during the years of low solar activity, a slight increase
in S corresponds to a small increase in the electron content. During
the periods of high solar activity when S has increased by a factor
of about three, the content increases by about a factor of about six.
The exact relationship between total content and the solar flux index
is not clear from this table because the data is grouped to either end
of the range. It does seem as though S is a more accurate indicator
of electron content during periods of low solar activity.

2. Seasonal Variation

Since the data being used cover a span from October to
March, it is unlikely that any strong seasonal effect will be
noticed. Nevertheless, it is seen from the two diurnal curves that
the midday values during February are approximately 5% to 10%
higher than those in November. It is also noticed that during

YEAR	LATITUDE	AUTHOR	ELECTRON CONTENT	S
1958	37.4°N	Garriott[13]	$7 \times 10^{17}/m^2$	250
1959	40.0°N	Yeh[24]	$7.5 \times 10^{17}/m^2$	225
1961	40.8°N	Hibberd[14]	$1.5 \times 10^{17}/m^2$	90
1963	43.0°N	Lyon[16]	$1.3 \times 10^{17}/m^2$	80
1964	40.8°N	Solomon	$0.95 \times 10^{17}/m^2$	73

ELECTRON CONTENT IN NOVEMBER

TABLE 1A

YEAR	LATITUDE	AUTHOR	ELECTRON CONTENT	S
1959	37.4°N	Garriott[13]	$7 \times 10^{17}/m^2$	200
1959	40.8°N	Ross[21]	$6 \times 10^{17}/m^2$	200
1962	40.8°N	Hibberd[14]	$1.5 \times 10^{17}/m^2$	100
1963	43.0°N	Lyon[16]	$1.3 \times 10^{17}/m^2$	80
1965	40.8°N	Solomon	$1.05 \times 10^{17}/m^2$	75

ELECTRON CONTENT IN FEBRUARY

TABLE 1B

November the values lie much closer to the curve with not nearly as much scattering as there is in February.

3. Gradients

Gradients will be measured by normalizing the average slope of an entire pass. In other words, the change in electron content per degree will be divided by the mean content for each pass so that the units of the gradient will be inverse degrees. This method will give the best basis for comparison among gradients from different passes.

The path of the satellite makes a 10.4° eastward angle with the meridian. This results in a 3 degree longitudinal difference in the ionosphere from one end of the path to the other (10° of latitude) which is equivalent to a thirteen minute difference in local time. Also, the satellite takes nine minutes to travel this path so that the electron content of the ionosphere at the ends of the pass is measured with a twenty-two minute difference in local time. This is much more important near sunrise when there is a large diurnal variation than at midday when a state of equilibrium between electron production and electron loss is nearly reached. The effect of this west-east gradient after sunrise will be discussed in the next section.

A study of all passes between 1800 in the evening and 0700 the following morning reveals that at these times there is generally a north-south gradient (content increases to the south) averaging 0.1; a few representative nighttime gradients are shown in Figure 6A.
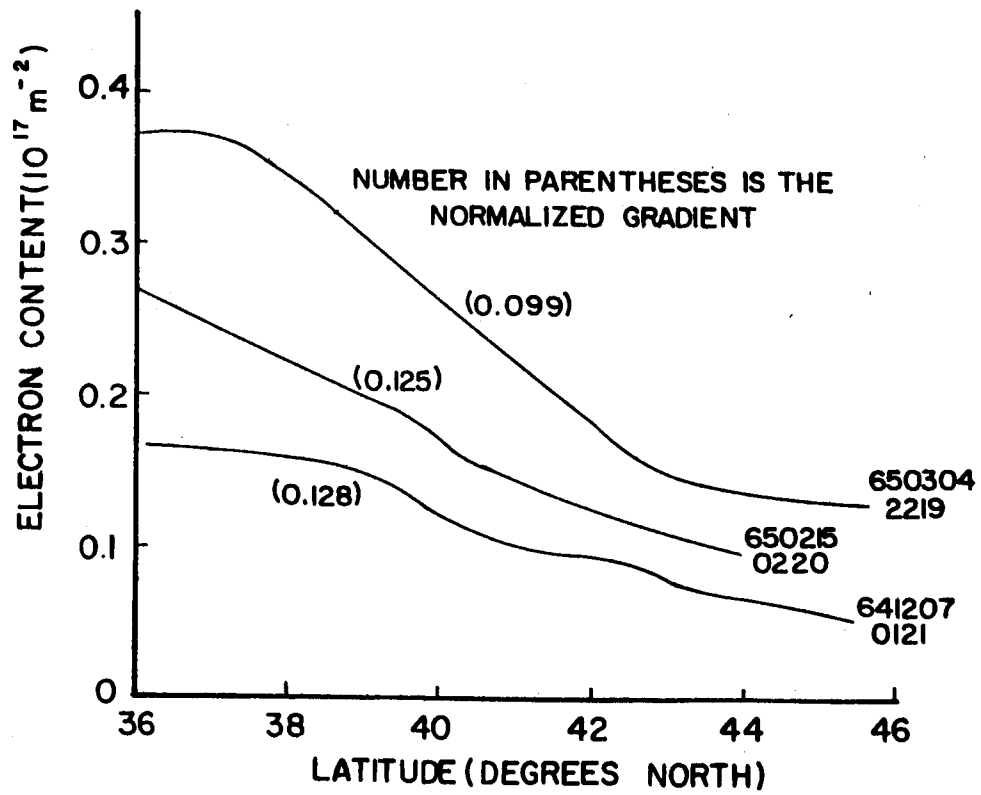
NIGHTTIME GRADIENTS

FIGURE 6A

In fact only a small number of passes between these times have virtually no gradient, and only three of them have s-n gradients. These three gradients are all rather small and exist only from the station northward. There is no obvious pattern to the magnitude of these gradients; they seem to be entirely unrelated to the values of the previous day.

The average value for daytime gradients between 1000 and 1800 is 0.01 which is ten times smaller than the nighttime value. The first group from the middle of October to the middle of December contains small gradients in either direction. Late afternoon passes are level for the most part with a few having a s-n gradient from the station northward. Two steep gradients from November passes are shown in Figure 6B. Their values of 0.022 and 0.045 are not nearly as high as nighttime values only because the mean value of electron content is so much higher. Around noon the gradient is n-s for the most part but it is not very large.

The northgoing passes are for times between 1000 and 1800 from the middle of January to the middle of March. These follow almost the same pattern as the southgoing passes with small gradients in the late afternoon, mostly n-s , and two spectacular deviations in February similar to those in November. The gradients gradually become predominantly n-s with an unexplained exception once in a while. As before, these exceptions are generally from the station northward.

All satellite passes between 0700 and 1000 in the morning
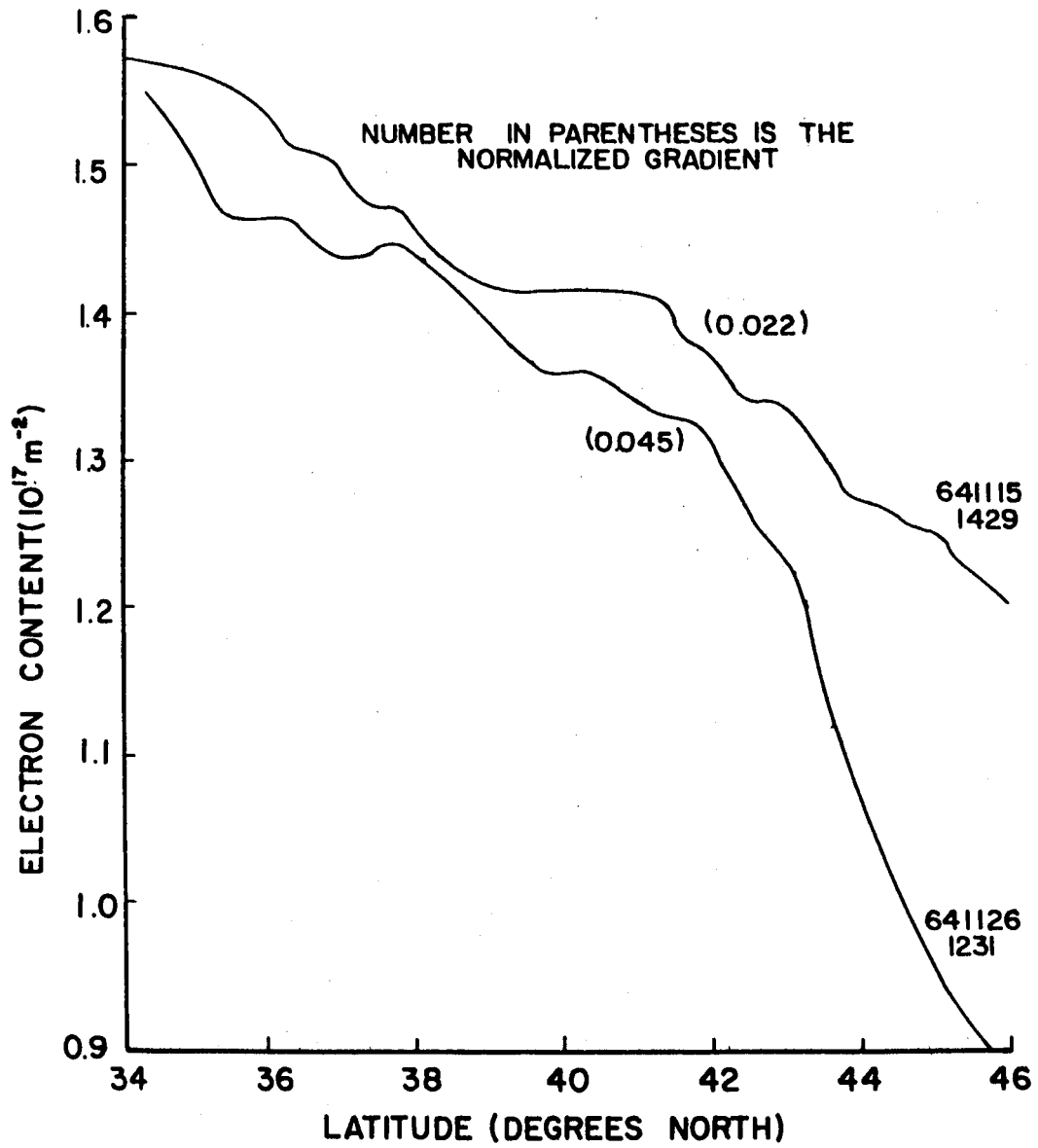
DAYTIME GRADIENTS

FIGURE 6B

have apparent n-s gradients, the average of the measured values being 0.058. This is about half the nighttime value, but only because of the higher magnitudes of electron content. The reasons for these gradients being much higher than the midday values will be seen in the following section.

The observations of nighttime gradients are in strong agreement with Butler[7] who has indicated a sharp increase in ionization toward the south during all seasons. For midday gradients he gets an average of zero for the fall and a slight s-n gradient for the winter. These results yield slight n-s gradients in November and February. One probable reason for the difference is that these data cover a larger geographical area. In many cases there is a s-n gradient from the station northward which is overshadowed by n-s gradients from the station southward. Thus, while the overall gradient is n-s , a ridge of electron content may very well exist to the north of the station. Curves of this nature are shown in Figure 7A.

Over the entire five months of passes, it is observed that many of the electron content vs. latitude curves seem to reach a local minimum just to the south of the station as in Figure 7A. The plot of these minimum points in Figure 7B shows that they are all located within two degrees latitude of the line drawn. This gives rise to the possibility that there is a trough to the south of the station.
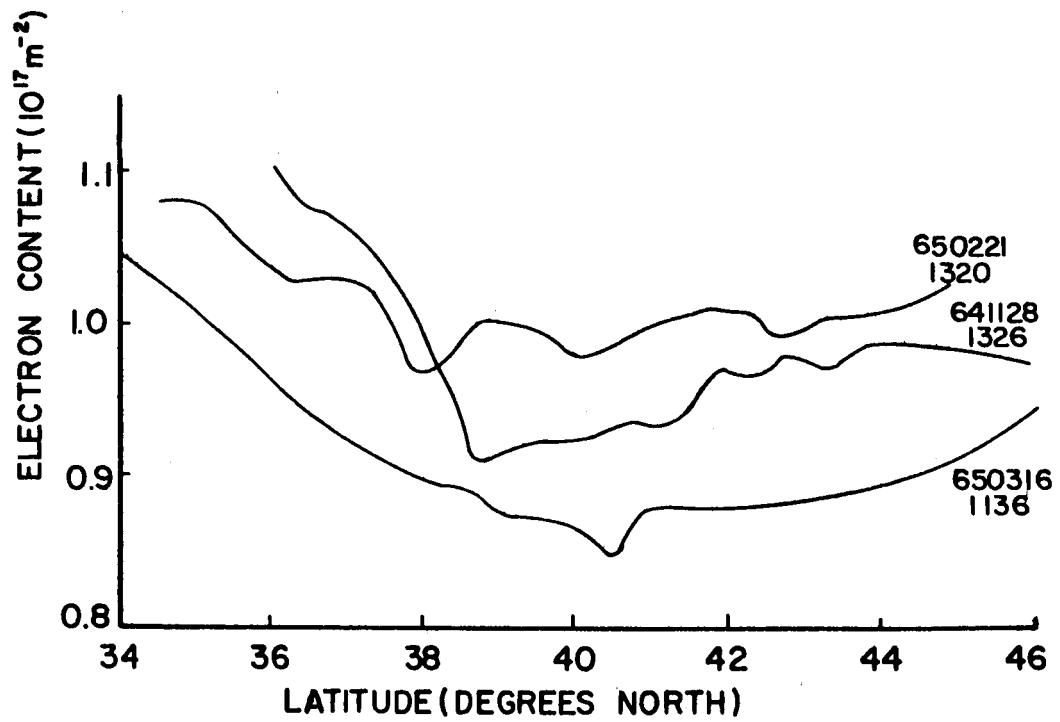
LOCAL MINIMUMS SOUTH OF THE STATION

FIGURE 7A
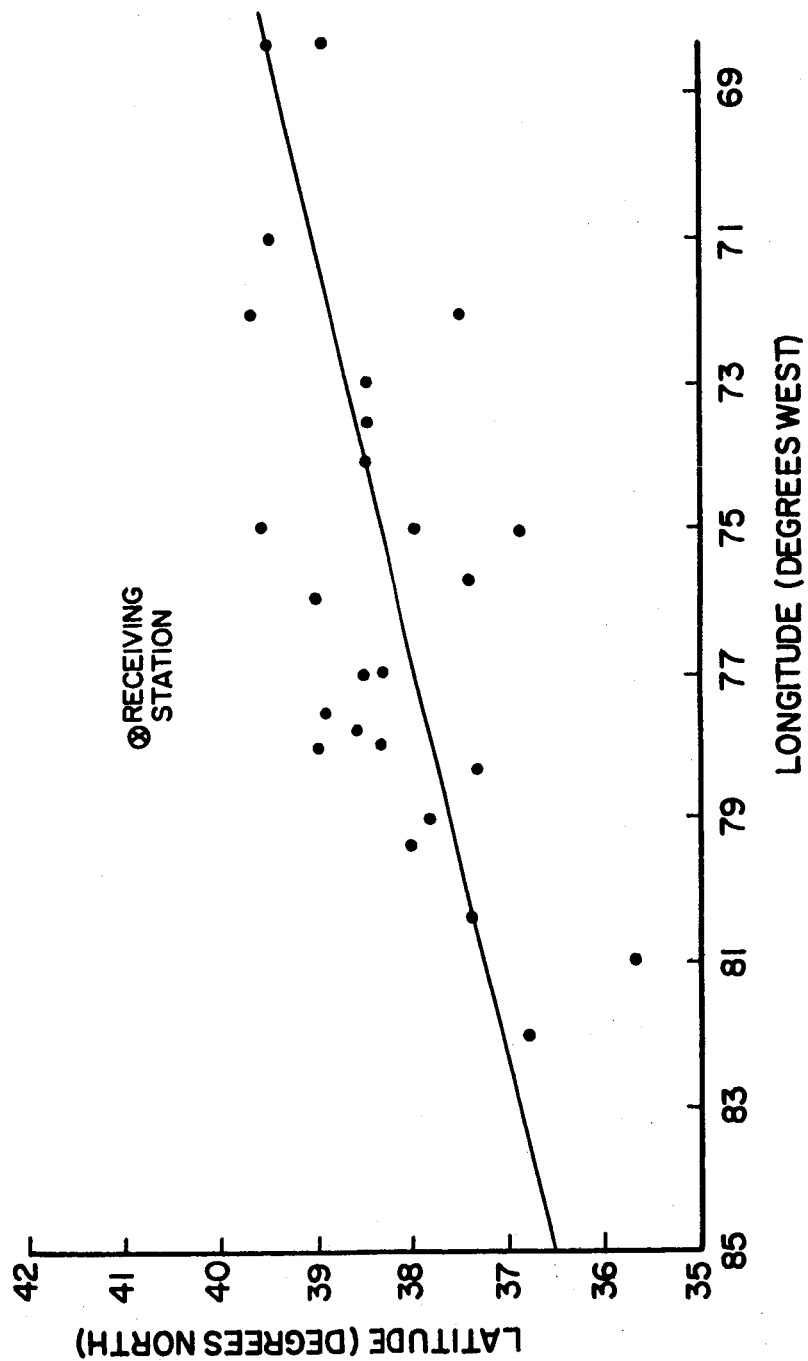
LOCATIONS OF LOCAL MINIMUMS IN ELECTRON CONTENT

FIGURE 7B

4. Sunrise Effects

In the morning from 0700 to 1000, the slope of the diurnal curve is 0.00285×10^{17} electrons per minute which is a difference of 0.063×10^{17} electrons for twenty-two minutes or ten degrees of ionosphere latitude. In other words, for the period immediately following sunrise, the longitudinal component of the satellite orbit and the travel time of the satellite are the source of a positive slope in the direction of travel of 0.0063×10^{17} electrons per degree.

For midday southgoing passes the average slope is 0.0112×10^{17} electrons per degree while the slope of electron content from southgoing passes from 0700 to 1000 is 0.0264×10^{17} electrons per degree. When the east-west effect is removed, the gradient becomes 0.47 instead of 0.58 and the slope reduces to 0.0201×10^{17} electrons per degree. This is almost a factor of two higher than the midday slope.

During the five months observations, sunrise was earlier to the south along a given meridian in the northern hemisphere. As a result, from sunrise on, the ionosphere to the south has been exposed for a longer period of time to the sun's ultraviolet rays which are the source of electron production. In the course of the day, this becomes negligible, but immediately after sunrise a pronounced effect is expected; i.e., there should be a large n-s gradient which gradually levels off to the midday value.

In Figure 8 there are curves from four passes when sunrise was at 0722 EST for $40°$N and $75°$W. The gradient is largest for the pass right around sunrise when the ionosphere below $40°$N has

NUMBER IN PARENTHESES IS
NORMALIZED GRADIENT

(0.045)

650103
0855

(0.067)

650101
0800

650104
0737

(0.076)

(0.2)

641231
0732
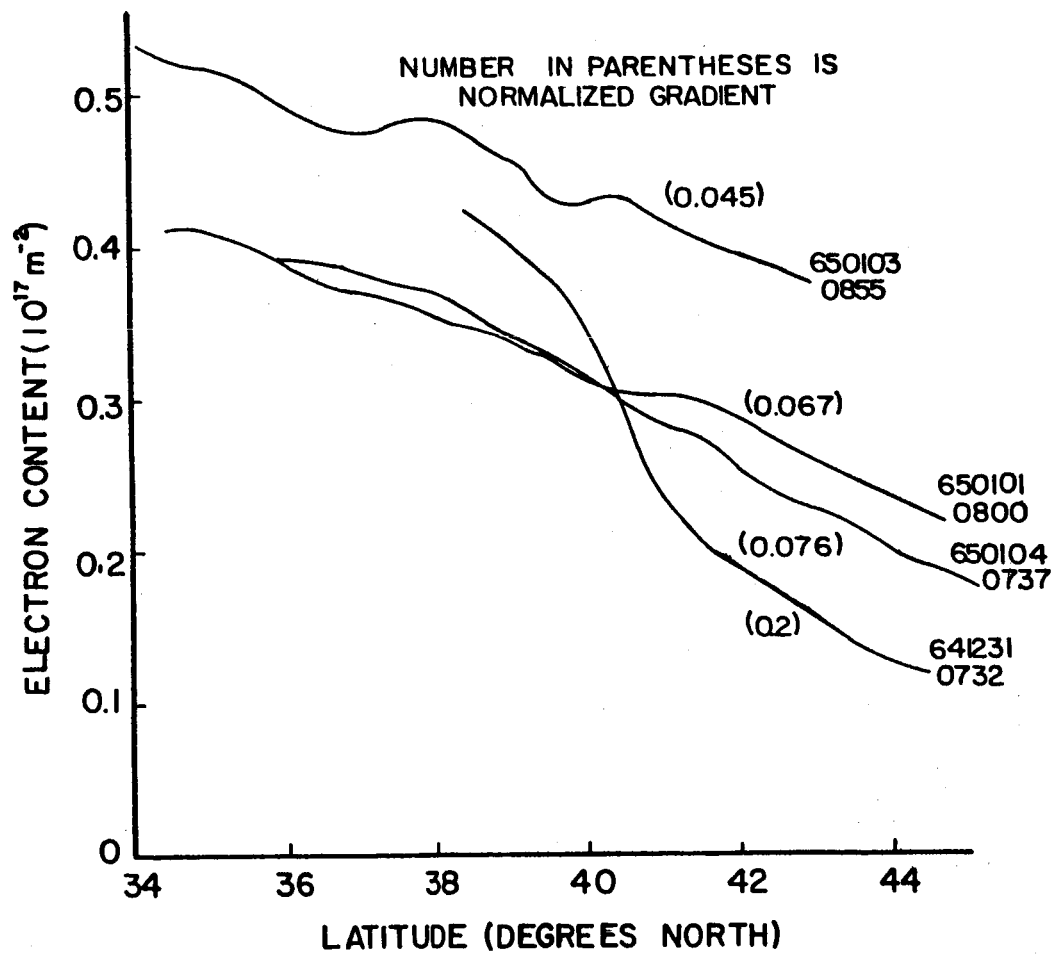
SATELLITE PASSES AFTER SUNRISE

FIGURE 8

already been exposed to the sun and that above 40°N has not. On the whole, the gradient decreases as expected.

During the end of December the difference between sunrise times at each end of a ten-degree satellite pass is thirty minutes. In the morning hours, this is equivalent to a difference of 0.0086×10^{17} electrons per degree of latitude. Since the average morning slope was shown to be 0.0201×10^{17} electrons per degree in the north-south direction, that part of the slope not contributed by the sunrise difference is 0.0115×10^{17} electrons per degree. This is essentially equal to the average midday slope of 0.0112×10^{17} electrons per degree.

5. Day-to-day Variation

Day-to-day variations are observed in total electron content as well as in the gradient. The variations are believed to be real and not due to random experimental error. The usual day-to-day variation is about 10% from the mean but occasionally there is an extremely large variation; this is generally in the form of an increase in electron content. The cause of these variations may be associated either with a variable electron production process or with the mechanisms of ionization removal or transfer.

The daily electron content at the station latitude is plotted in Figures 9A and 9B for two large intervals of time. In both graphs the value nearest to noon was used when there were two day-time values; the approximate times are shown. Below each curve is a plot of the planetary magnetic disturbance index for each
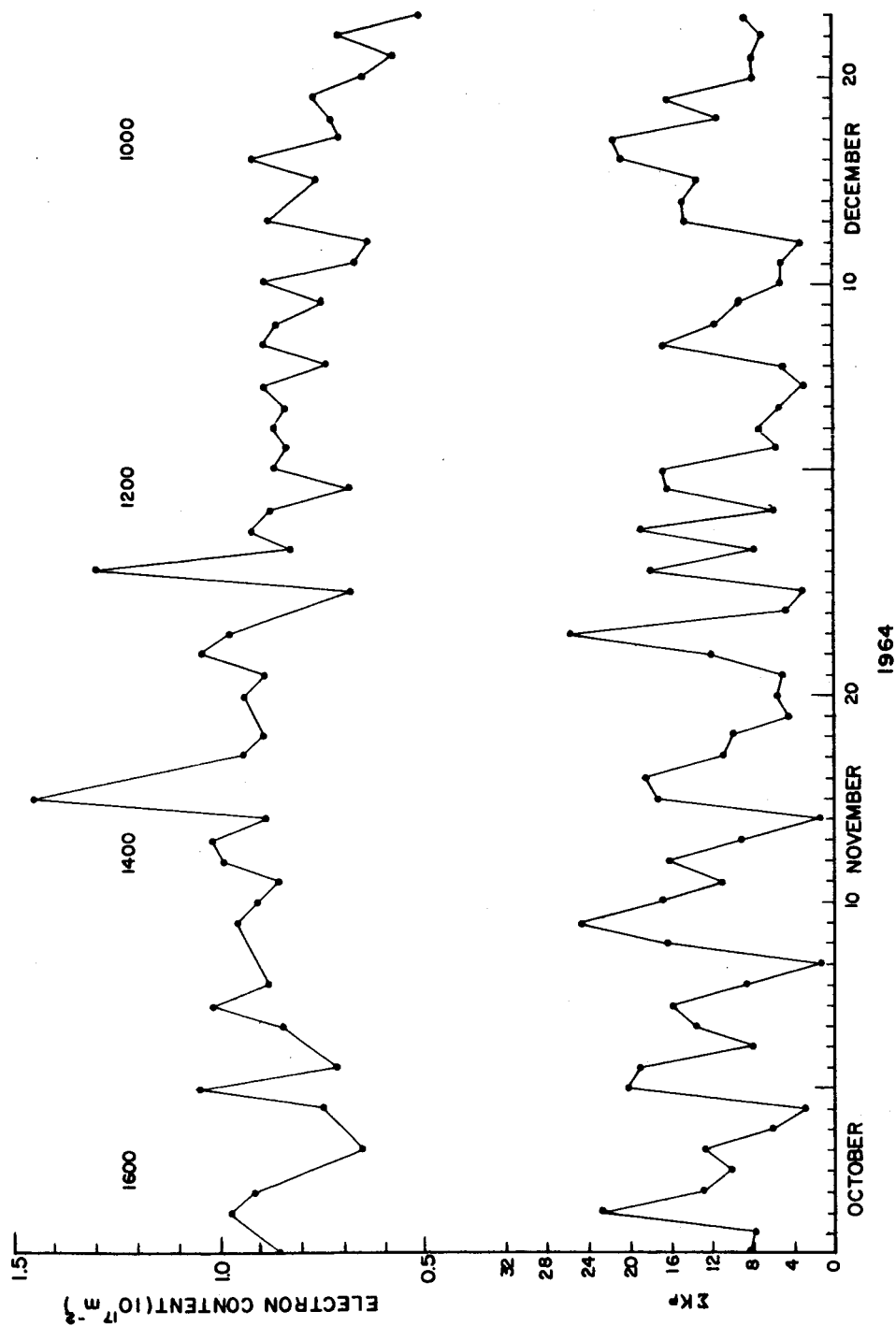
COMPARISON OF ELECTRON CONTENT WITH 24 HOUR PLANETARY INDEX Kp

FIGURE 9A
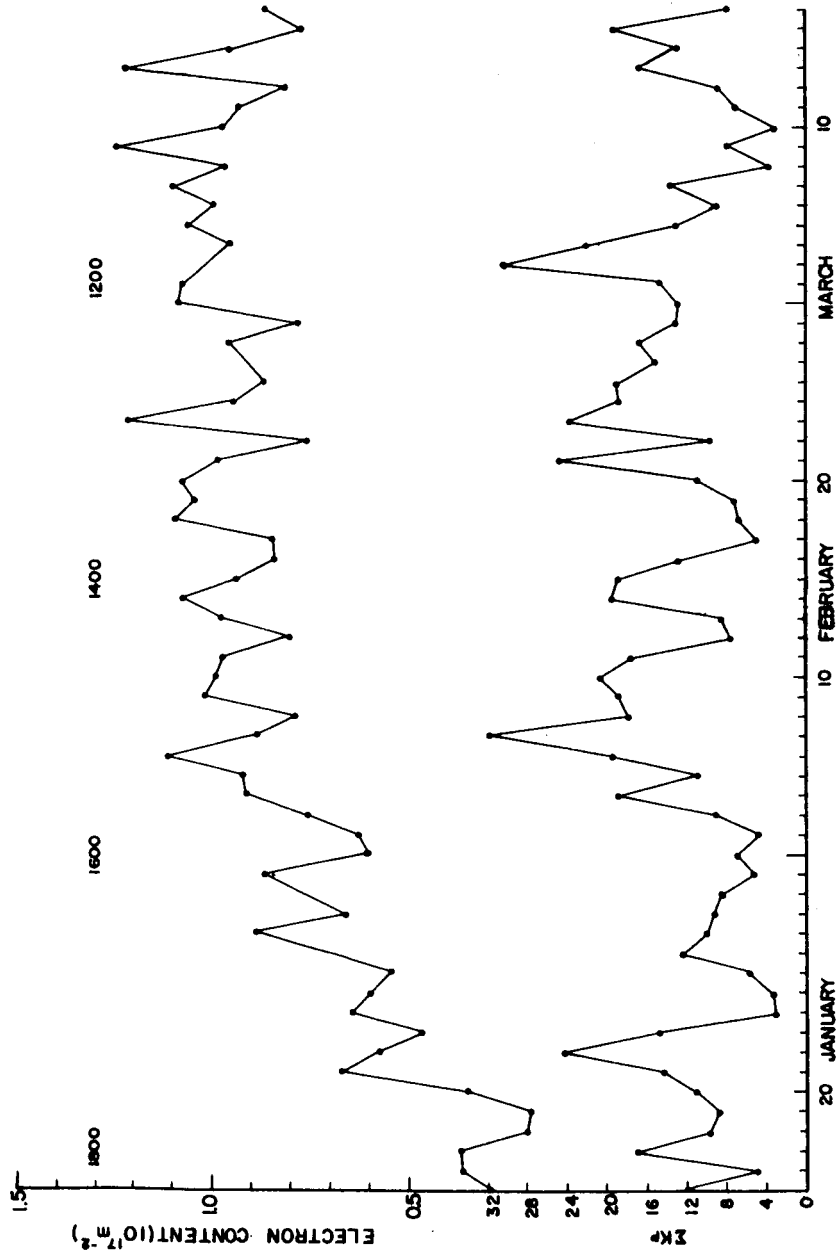
COMPARISON OF ELECTRON CONTENT WITH 24 HOUR PLANETARY INDEX Kp

FIGURE 9B

day. The upper curve clearly shows the day-to-day variations;
care must be taken to distinguish diurnal from daily variations.
The beginning of Figure 9B is in the late afternoon when the diurnal
variation is rapid. Since the times of observation vary each day,
daily variations are inaccurate at those times when the diurnal
variation is large. During the middle of the day, however, the
observation time will not be as important.

An attempt is made to correlate variations in electron con-
tent with magnetic activity as measured by the planetary magnetic
index K_p. This index is calculated for eight 3-hour intervals every
day. Figures 9A and 9B show no readily apparent correlation
between the two quantities in question. This is in line with the
results of Ross[21] and Garriott[13] who found no systematic
dependence during the winter months although both Ross and Lyon[16]
have shown an inverse relationship during the summer months.

Individual passes where the electron content has undergone
a large variation from the mean or expected value are now examined.
The behavior of K_p for the period preceding the pass will then be
discussed. (Unless stated otherwise, ΣK_p will refer to the 24
hours before the pass, and all times will be in Eastern Standard
Time.)

The first group of passes are shown in Figure 10. All but
one of them have steep n-s gradients and the magnitudes of the
electron content are considerably higher than those of other days.
Previous to the two November 15 passes, $\Sigma K_p = 4-1/3$ for the
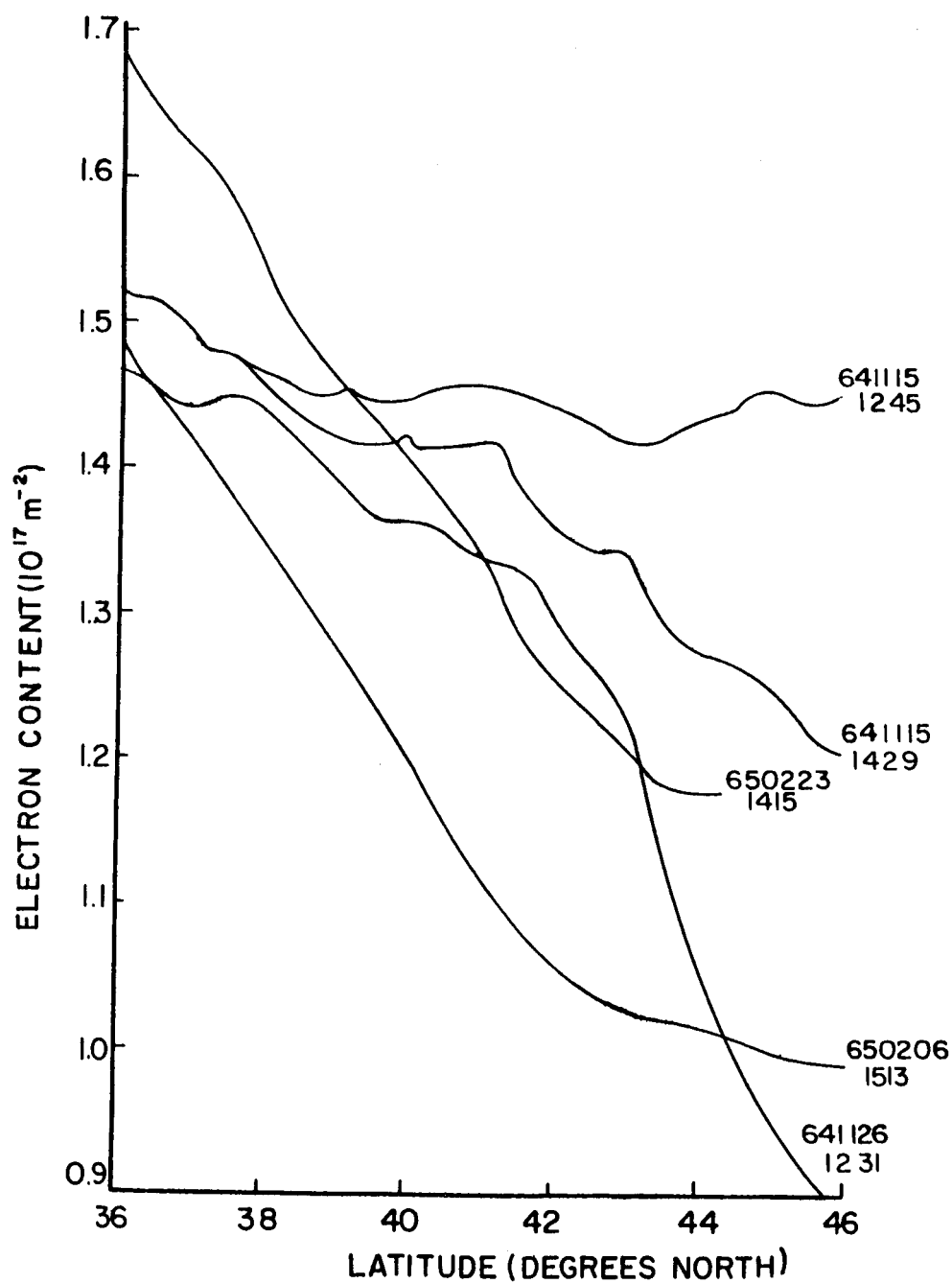
STEEP N-S GRADIENTS AND LARGE ELECTRON CONTENT

FIGURE 10

period from 1300 on November 13 to 0700 on November 15. Then the value of K_p immediately rose to between 3 and 4 through the times of the passes at 1245 and 1429. The run of November 26 at 1231 was also preceded by a quiet period, but earlier that day K_p went up to over 3. On February 6 there was a sudden commencement between 0700 and 1000 and K_p went up to 4-2/3 for the next three hours; the pass was two hours later at 1513. Another pass which was 105 minutes later yielded normal results. The final pass of the set on February 23 at 1415 was characterized by K_p = 4-1/3 from 1000-1300 and K_p = 4-2/3 from 1300-1600. Also there had been a sudden commencement at 0600. The previous pass at 1230 showed an electron content which was slightly higher than normal and a small s-n gradient. Further sets of results will be examined before attempting to draw any conclusions.

In Figure 11 there are three early afternoon passes whose magnitudes are somewhat low for that particular time of day. Preceding the November 25 pass, ΣK_p = 1-1/3 which is extremely low. On the other hand, for the November 30 pass ΣK_p = 18, and ΣK_p = 11 before the February 22 pass. There certainly cannot be any correlation inferred from this set of results.

The electron content curves in Figure 12 are slightly higher than usual in magnitude with a substantial s-n gradient. For the November 22 pass, ΣK_p = 11-1/3 which is not an unusual value. Similarly, ΣK_p = 12-1/3 before the March 2 results and ΣK_p = 6-2/3,
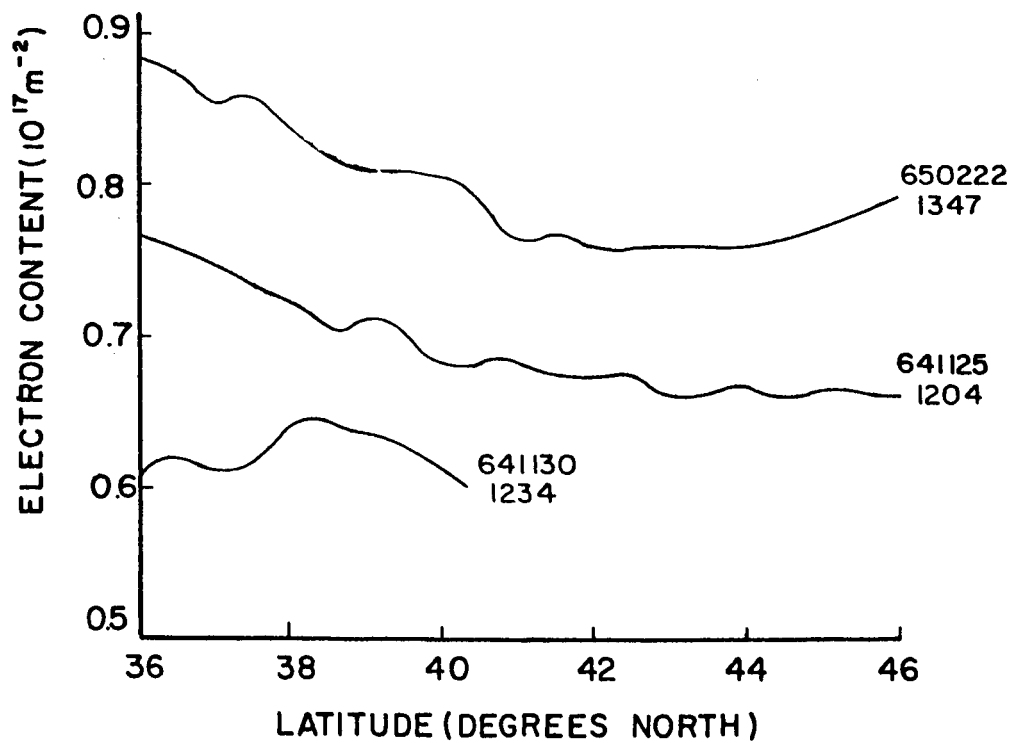
EARLY AFTERNOON PASSES DISPLAYING
SMALL ELECTRON CONTENT

FIGURE II
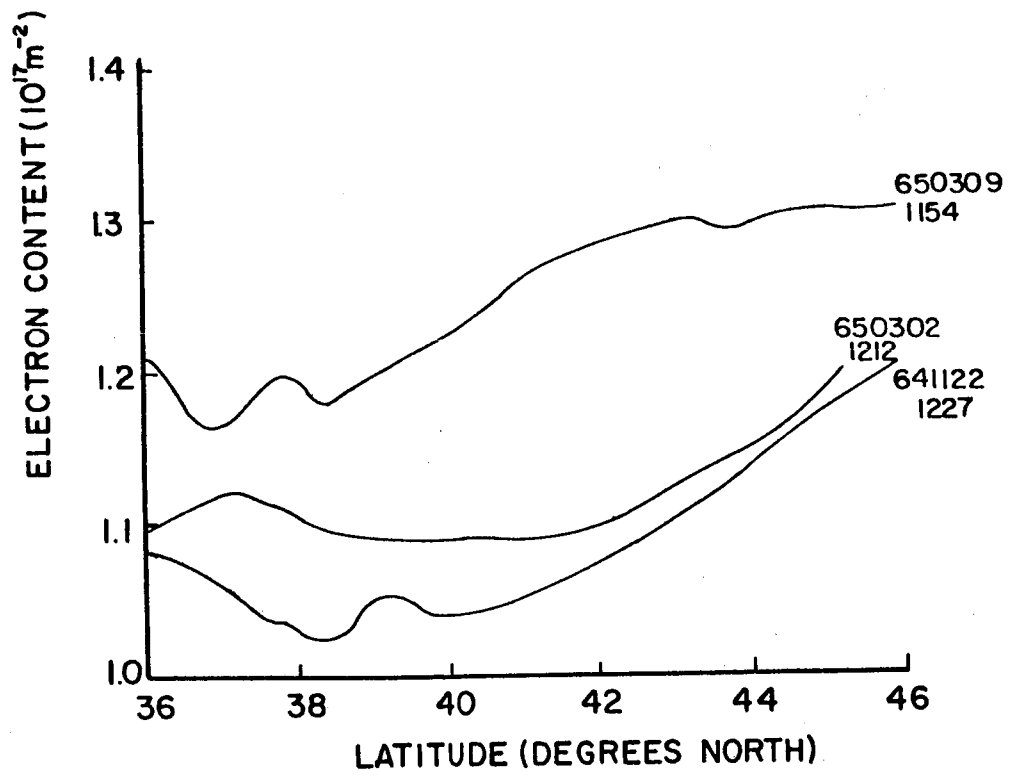
S-N GRADIENTS

FIGURE 12

a low value, before the March 9 pass. Once again there is no clear relationship to be found.

The three passes shown in Figure 13 have relatively steep n-s gradients although the magnitudes of their electron contents are as expected. The December 16 run at 0925 is characterized by K_p being equal to 5-1/3 during the period from 0700-1000. For the March 4 passes, ΣK_p = 29-1/3 which is a relatively large index.

Figure 14 shows passes displaying unusual behavior at night. The early morning pass on December 5 had a higher electron content than would be expected for that time and was associated with a relatively low value of ΣK_p = 7-2/3. Prior to the January 22 pass at 0521, K_p = 5-2/3 from 0100 to 0400, and before the March 3 pass at 2336, K_p = 6 from 2200 to 0100 the next day. Both of these curves have steep n-s gradients.

It seems as though there might be an association between the electron content and the magnetic activity. For both sets of afternoon passes having steep n-s gradients, K_p had risen up to between three and six before each of these passes. Other daytime passes which follow times when K_p rises to over three are examined. Four of the six passes in this category showed either a higher electron content than usual or a reasonably steep gradient; the other two had average results.

Re-examining the nighttime results, it is noticed that the passes with steep n-s gradients were preceded by high values of K_p. Checking back through the entire five months, it is seen that
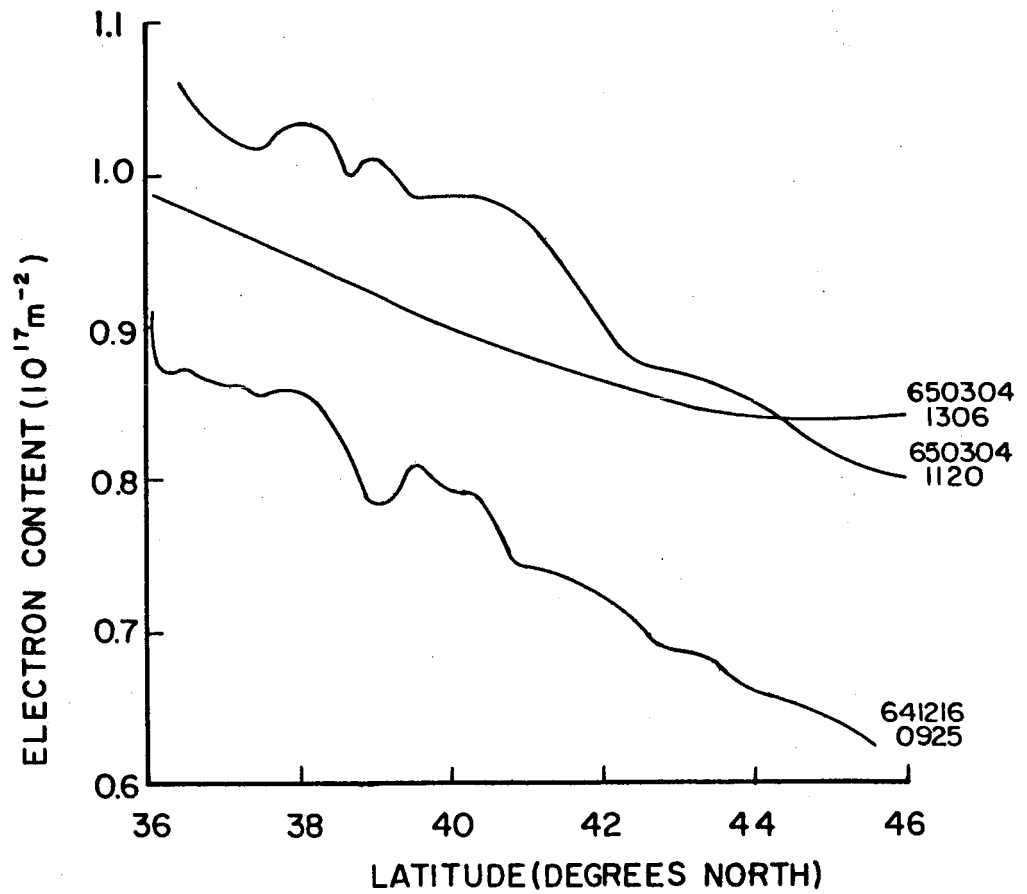
STEEP N-S GRADIENTS

FIGURE 13
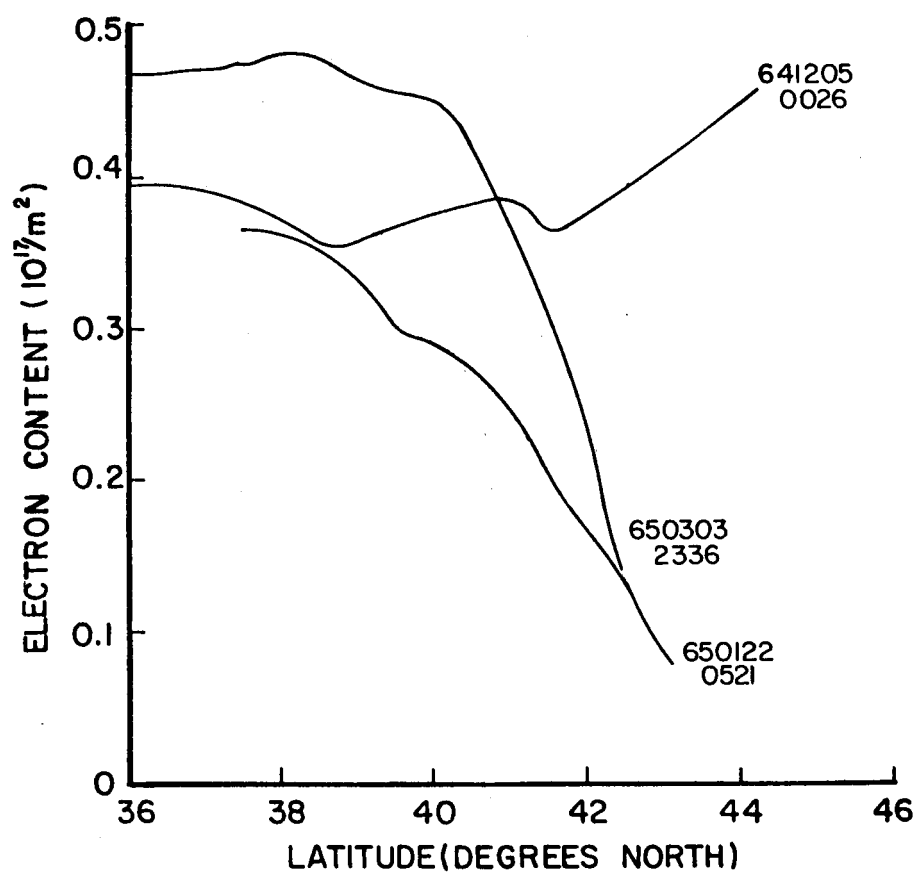
UNUSUAL BEHAVIOR AT NIGHT

FIGURE 14

every time the value of K_p rises above five, there is a steep n-s gradient in the plot of the following nighttime pass.

For both the day and night there is an association of magnetic activity with horizontal north-south gradients in the electron content. This gradient is a result of an increase in electron content to the south and/or a decrease to the north. If the agency responsible for magnetic disturbances increases the temperature of the upper atmosphere to the north there would be a corresponding increase in the vertical transport of oxygen molecules. This in turn would increase the recombination rate, thereby causing a decrease in content to the north.

VI. SUMMARY

1. <u>Conclusions</u>

Studies of the variation of the total electron content of the ionosphere at mid-latitudes have been made based on data taken at University Park, Pennsylvania (40.8°N, 77.9°W) from October 24, 1964 to March 16, 1965. The S-66 Beacon Satellite has been used for all observations, and the equipment used for analysis has been described.

Values for $\overline{B \cos \theta \sec \chi}$ were precomputed and the method of unambiguously determining the number of rotations of the plane of polarization of the 41 MHz signal has been discussed. The total electron content was then calculated using this data, with precautionary measures being taken to keep the error to a minimum.

The horizontal gradients are generally positive from north to south averaging 0.1 per degree at night, 0.047 per degree in the morning, and 0.01 per degree during the day. Morning results have been corrected for west-east slopes resulting from the eastward direction of the satellite path and the travel time of the satellite from one end of the observed path to the other. The contribution of an earlier sunrise in the south has also been determined.

There was a large diurnal variation as expected with the ratio of daytime maximum to nighttime minimum being between 5 and 10 to 1. In February, the maximum values of electron content occur slightly earlier in the day and are 5% to 10% higher than those in November. A comparison between electron content

results during periods of high and low solar activity showed that when the value of the solar flux index was a factor of about three higher the electron content was larger by a factor of about six.

Day-to-day variations averaging about 10% were observed in the total electron content. There was no systematic dependence between the planetary magnetic disturbance index and the magnitude of the electron content. It was noted that following increases in magnetic activity, there were increases in the horizontal north-south gradients for both the day and the night. The decrease of content to the north is believed to be the result of an increase in the recombination rate at higher latitudes.

The locations of local minimums in electron content led to the observation of an apparent trough just to the south of the station.

2. Suggestions for Further Work

The data presented here were observed over a five-month interval. Seasonal effects on the total electron content and its horizontal gradient cannot be deduced until results are calculated for the remaining seven months of the year. Calculations at times when there is more magnetic activity, will aid in determining a correlation with electron content. Observations must be made continuously over a period of years to ascertain the solar cycle variation.

Dispersive doppler results should be computed and compared with Faraday rotation results; this would be of use in the

investigation of irregularities. The possible trough to the south of the station should be verified by further studies.

An improvement in the determination of the mean ionosphere height at which to evaluate the geomagnetic field would increase the accuracy of the Faraday rotation method.

BIBLIOGRAPHY

1. Aitchison, G. J. and K. Weekes - "Some Deductions of Ionospheric Information from the Observations of Emissions from Satellite 1957 α2 - I, II", JATP, 14, p. 236 (1959).

2. Blackband, W. T., B. Burgess, I. L. Jones, and G. J. Lauson - "Deduction of Ionospheric Electron Content from the Faraday Fading of Signals from Artificial Earth Satellites", Nature, 183, p. 1172, (1959).

3. Blumle, L. J. - "Satellite Observations of the Equatorial Ionosphere", JGR, 67 (12), p. 4601, (1962).

4. Booker, H. G. - "The Application of the Magneto-Ionic Theory to the Ionosphere", Proc. Roy. Soc., 150, p. 267, (1935).

5. Bowhill, S. A. - "The Faraday Rotation Rate of a Satellite Radio Signal", JATP, 13, p. 175, (1958).

6. Browne, I. C., J. V. Evans, J. K. Hargreaves, and W. A. S. Murray - "Radio Echoes from the Moon", Proc. Phys. Soc., 69, p. 901, (1956).

7. Butler, H. W. -"An Investigation of Horizontal Gradients in the Electron Content of the Ionosphere", Ionosphere Research Laboratory, The Pennsylvania State University, Sci. Report No. 165, (1962).

8. Daniels, F. B. - "Electromagnetic Propagation Studies with a Satellite Vehicle", in "Scientific Uses of Earth Satellites" by J. A. VanAllen, p. 276, (1956).

9. Daniels, F. B. and S. J. Bauer - "The Ionospheric Faraday Effect and its Applications", USASRDL Technical Report 1980, (1958).

10. Daniels, F. B. and S. J. Bauer - "Measurement of the Ionospheric Faraday Effect by Radio Waves Reflected from the Moon", Nature, 181, p. 1392, (1958).

11. Evans, J. V. - "The Measurement of the Electron Content of the Ionosphere by the Lunar Radio Echo Method", Proc. Phys. Soc. B, 69, p. 953, (1956).

12. Evans, J. V. - "The Electron Content of the Ionosphere", JATP, 11, p. 259, (1959).

13. Garriott, O. K. - "The Determination of Ionosphere Electron Content and Distribution from Satellite Observations", JGR, 65 (4), p. 1139, (1960).

14. Hibberd, F. H. - "A Study of the Ionosphere at Mid-Latitudes Based on Total Electron Content", Ionosphere Research Laboratory, The Pennsylvania State University, Sci. Report No. 213, (1964).

15. Kelso, J. M. - "Radio Ray Propagation in the Ionosphere", McGraw-Hill Inc., (1964).

16. Lyon, G. F. - "Satellite Transmission Measurements of Ionospheric Electron Content at a Time of Low Solar Activity", Canadian Journal of Physics, 43, p. 1059, (1965).

17. Mullard Radio Astronomy Observatory - "Radio Observations of the Russian Earth Satellite", Nature, 180, p. 882, (1958).

18. Murray, W.A.S. and J. K. Hargreaves - "Lunar Radio Echoes and the Faraday Effect in the Ionosphere", Nature, 173, p. 944, (1954).

19. Ratcliffe, J. A. - "The Magneto-Ionic Theory and its Applications to the Ionosphere", University Press, Cambridge, (1959).

20. Ratcliffe, J. A. - "Physics of the Upper Atmosphere", Academic Press, (1960).

21. Ross, W. J. - "The Determination of Ionospheric Electron Content from Satellite Doppler Measurements 2. Experimental Results", JGR, 65 (9), p. 2607, (1960).

22. Ross, W. J. - "Second-order Effects in High-frequency Transionospheric Propagation", JGR, 70 (3), p. 597, (1965).

23. Swenson, G. W. Jr. - "The Utilization of Ionosphere Beacon Satellites", Publication X-250-62-32, Goddard Space Flight Center, (1962).

24. Yeh, K. C. and G. W. Swenson Jr. - "Ionospheric Electron Content and its Variations Deduced from Satellite Observations", JGR, 66 (4), p. 1061, (1961).

APPENDIX

Experimental Data

The following tabulations of data list the more important quantities derived from the satellite passes which have been analyzed. For each pass, a null was picked at the time closest to when the satellite crossed the station latitude. The height of the satellite is given at the time of this null, along with the latitude and longitude of the ionosphere point, which determines the location of the vertical meter square column for which the electron content is calculated. The results are given in chronological order with the following notation.

DATE - date of record in Eastern Standard Time

TIME - time of the null in Eastern Standard Time

HEIGHT - height of the satellite in Km at TIME

LONG - longitude of the meter square column in degrees west

LAT - latitude of the meter square column in degrees north

$\int Ndh$ - electron content of the meter square column up to HEIGHT in units of 10^{17} .

DATE	TIME	HEIGHT	LONG	LAT	$\int$ Ndh
641024	1640:49	906	76.07	40.87	0.851
641026	1550:47	910	73.10	40.98	0.982
641026	1736:10	912	81.66	40.29	0.531
641027	1617:53	912	76.30	41.10	0.920
641029	1712:51	919	81.90	40.98	0.647
641031	1622:45	924	79.10	40.88	0.753
641101	1505:19	927	73.59	41.03	1.079
641102	1717:45	931	85.93	41.05	0.711
641104	1627:27	937	82.18	41.02	0.848
641105	1509:45	939	76.79	41.12	1.022
641105	1655:14	942	86.17	40.83	0.843
641106	0441:26	909	78.34	41.30	0.198
641106	1352:54	946	70.01	40.93	0.878
641106	1537:24	945	79.36	40.86	0.985
641107	0323:18	908	72.68	40.78	0.154
641107	0508:02	909	81.49	40.60	0.230
641108	0341:08	906	75.81	41.10	0.163
641109	1330:03	956	70.46	41.11	0.972
641109	1514:28	954	79.54	41.11	0.924
641110	1357:14	959	74.25	41.03	0.913
641110	1542:14	960	82.43	40.89	0.819
641111	0328:08	901	76.01	40.79	0.240
641111	1424:31	963	77.06	40.98	0.862
641112	0355:24	900	78.81	40.67	0.159
641112	1451:54	967	79.65	41.02	0.994
641113	0238:04	898	73.00	40.97	0.218
641113	1334:33	972	74.46	41.02	1.020
641113	1519:30	973	82.56	40.96	0.893
641114	1547:08	978	86.58	41.00	0.884
641115	0332:34	896	79.00	40.55	0.172
641115	1244:34	980	71.19	41.21	1.454
641115	1429:24	980	79.74	40.85	1.416
641116	0215:10	895	73.20	40.75	0.206
641117	1339:05	987	77.38	41.06	0.940
641118	1222:03	993	71.39	41.03	0.895
641118	1406:27	991	79.92	41.13	0.950
641119	0152:47	894	73.34	41.12	0.165
641119	0337:54	894	81.92	41.45	0.193
641120	0219:45	893	76.51	40.54	0.177
641120	1316:28	1000	77.51	41.02	0.940
641121	0102:10	893	69.47	40.76	0.248
641121	0246:52	893	79.39	40.27	0.143
641121	1149:32	1007	71.61	40.88	0.878
641121	1343:51	1004	80.03	41.07	0.856
641122	1226:41	1009	75.00	40.88	1.050
641123	0157:26	894	76.57	40.97	0.134
641123	1253:56	1013	77.62	40.91	0.976
641125	1203:47	1020	75.26	41.09	0.678

DATE	TIME	HEIGHT	LONG	LAT	$\int Ndh$
641126	1231:24	1026	77.72	40.80	1.343
641127	1114:02	1029	72.26	41.05	0.913
641127	1258:31	1028	80.28	41.12	0.820
641128	1141:12	1032	75.42	41.03	0.868
641128	1326:07	1032	83.25	41.16	0.932
641129	0112:18	902	76.80	41.29	0.053
641129	1208:24	1035	77.97	41.13	0.873
641130	1051:11	1040	72.62	41.23	0.967
641130	1234:12	1047	78.73	40.31	0.653
641201	0021:28	903	74.17	40.58	0.206
641201	1303:41	1045	83.37	40.95	0.875
641202	1146:12	1048	78.01	40.74	0.841
641203	1028:43	1050	72.77	41.05	0.758
641203	1213:37	1051	80.48	40.78	0.871
641204	1056:03	1053	75.71	40.90	0.782
641204	1240:45	1053	83.54	41.28	0.836
641205	0026:36	914	77.17	40.99	0.388
641205	1123:35	1057	78.13	40.73	0.895
641205	2312:06	938	67.13	36.75	0.067
641206	1006:06	1060	73.00	41.03	0.696
641206	1150:45	1059	80.64	41.02	0.742
641206	2337:07	922	74.37	41.76	0.145
641207	0120:35	916	83.48	40.40	0.112
641207	1033:31	1063	75.84	40.80	0.831
641207	1218:18	1063	83.68	41.11	0.894
641207	0003:51	921	77.32	40.95	0.212
641208	1100:49	1064	78.28	40.85	0.853
641209	0943:33	1068	73.17	40.93	0.636
641209	1128:04	1067	80.78	41.08	0.750
641210	0058:38	928	83.18	41.26	0.197
641210	1155:31	1070	83.86	41.30	0.902
641211	1037:59	1071	78.45	41.04	0.676
641212	1105:31	1073	80.91	41.03	0.636
641213	0947:52	1075	76.25	41.14	0.606
641213	1132:49	1075	84.04	41.41	0.884
641214	1015:30	1077	78.55	40.91	0.816
641214	2200:43	943	71.72	40.95	0.187
641215	0858:12	1078	73.61	41.00	0.674
641215	1042:58	1079	81.03	40.97	0.768
641215	2228:38	950	75.02	41.30	0.112
641216	0925:23	1079	76.36	41.03	0.741
641216	1110:44	1080	84.19	40.86	0.936
641217	0952:57	1081	78.67	40.86	0.709
641218	0835:39	1082	73.76	40.92	0.537
641218	1020:08	1081	81.21	41.19	0.733
641219	0902:58	1082	76.44	40.84	0.712
641219	1048:10	1083	84.39	40.83	0.779

DATE	TIME	HEIGHT	LONG	LAT	$\int Ndh$
641219	2233:00	965	77.95	40.89	0.112
641220	0930:06	1083	78.84	41.06	0.646
641220	2115:31	968	72.27	41.12	0.107
641220	2259:43	965	80.83	40.30	0.140
641221	0812:43	1083	74.07	41.21	0.428
641221	0957:30	1083	81.37	41.22	0.579
641222	0840:05	1084	76.66	41.08	0.452
641222	1025:35	1083	84.62	40.83	0.728
641222	2211:25	985	77.76	41.93	0.113
641223	0907:42	1083	78.94	40.88	0.515
641229	2007:16	1004	73.04	40.82	0.185
641229	2152:38	1008	80.83	41.24	0.163
641230	0704:54	1079	74.52	41.14	0.216
641230	0850:14	1077	81.81	40.71	0.384
641230	2034:36	1008	76.01	41.61	0.180
641231	0732:33	1076	76.97	40.80	0.252
641231	0917:24	1077	85.35	41.24	0.565
641231	2102:18	1014	78.46	40.87	0.176
650101	0800:10	1075	79.30	40.62	0.304
650101	1944:47	1018	73.27	41.00	0.191
650102	0827:04	1074	82.04	41.25	0.436
650102	2012:09	1021	76.14	40.80	0.305
650102	2157:15	1024	84.25	41.44	0.209
650103	0855:12	1069	85.64	40.81	0.420
650103	2040:05	1029	78.49	41.27	0.175
650104	0737:16	1069	79.50	40.88	0.286
650104	1922:04	1029	73.51	40.92	0.240
650104	2106:21	1026	81.49	40.34	0.165
650105	0805:05	1065	82.19	40.63	0.327
650105	1950:34	1039	76.11	41.78	0.198
650106	0647:27	1063	77.20	40.67	0.203
650106	0832:07	1064	85.94	41.34	0.397
650106	2017:54	1042	78.50	41.67	0.145
650107	0714:47	1061	79.62	40.75	0.194
650107	2044:51	1044	81.14	41.42	0.257
650108	1927:31	1048	76.32	41.38	0.193
650109	1809:27	1047	70.33	41.28	0.376
650110	0507:12	1053	71.88	41.19	0.293
650110	0534:25	1050	75.06	41.09	0.199
650111	1904:16	1054	76.59	40.82	0.274
650112	0602:24	1044	77.41	40.47	0.088
650112	1746:37	1055	70.63	41.02	0.493
650112	1932:18	1059	78.83	41.38	0.268
650113	0444:29	1044	73.08	41.25	0.163
650113	0629:32	1042	79.93	40.74	0.149
650113	1814:05	1059	74.12	40.82	0.334
650113	1959:02	1060	81.62	40.93	0.203

DATE	TIME	HEIGHT	LONG	LAT	$\int$ Ndh
650114	0511:58	1039	75.11	40.91	0.149
650114	1842:08	1065	76.65	41.26	0.165
650115	0539:09	1037	77.67	41.00	0.198
650115	1724:06	1064	70.91	41.12	0.289
650115	1909:15	1066	79.06	41.02	0.188
650116	0606.05	1036	80.22	41.51	0.165
650116	1751:27	1066	74.31	40.80	0.363
650116	1937:04	1070	81.49	41.55	0.224
650117	0449:27	1027	75.20	40.79	0.221
650117	0634:19	1027	83.09	40.90	0.165
650117	1819:04	1070	76.88	40.87	0.371
650117	2003:04	1067	85.82	40.51	0.326
650118	1846:48	1073	79.15	41.17	0.191
650119	0359:27	1019	72.20	40.95	0.227
650119	0544:59	1014	80.18	40.04	0.203
650119	1914:52	1078	81.47	41.94	0.188
650120	0426:34	1017	75.41	40.99	0.200
650120	0611:56	1013	83.34	40.62	0.159
650120	1756·34	1077	76.99	40.97	0.356
650121	0453:16	1016	78.10	41.55	0.182
650121	1638:38	1077	71.44	40.86	0.673
650121	1823:52	1078	79.36	40.90	0.404
650122	0336:52	1007	72.29	40.85	0.157
650122	0521:02	1011	80.52	41.28	0.221
650122	1706:22	1079	74.64	40.93	0.574
650122	1851:26	1080	81.94	41.23	0.282
650123	0403:37	1006	75.63	41.25	0.225
650123	0549:28	1000	83.61	40.43	0.200
650123	1733:49	1080	77.15	40.86	0.462
650123	1918:17	1080	85.87	41.05	0.267
650124	0432:05	996	77.94	40.17	0.094
650124	1616:03	1081	71.67	40.87	0.643
650125	0458:33	997	80.68	41.12	0.116
650125	1644·00	1083	74.78	41.15	0.601
650125	1828·30	1082	82.24	40.95	0.343
650126	0340:41	996	75.83	41.50	0.141
650126	0526:27	989	83.89	40.82	0.216
650126	1711:22	1083	77.24	41.01	0.549
650128	0436:19	982	80.81	40.69	0.171
650128	1621:20	1083	74.93	41.10	0.895
650128	1805:55	1084	82.39	41.01	0.640
650129	0318:13	982	75.88	41.29	0.160
650129	1648:58	1084	77.33	41.19	0.662
650130	1531:10	1084	73.08	41.20	0.776
650131	0229:04	968	72.55	40.56	0.138
650131	0413:20	971	81.05	41.01	0.159
650131	1558:44	1084	75.08	41.11	0.870

DATE	TIME	HEIGHT	LONG	LAT	$\int$ Ndh
650131	1743:26	1084	82.51	41.14	0.657
650201	0255:26	970	76.04	41.38	0.230
650201	1625:50	1084	77.56	40.75	0.606
650201	1811·06	1084	86.08	41.83	0.525
650202	0138:48	961	68.57	41.11	0.331
650202	0323:26	962	78.46	40.74	0.189
650202	1653:15	1083	79.95	40.82	0.627
650203	0350:18	961	81.29	41.37	0.174
650203	1536:11	1082	75.21	41.16	0.757
650203	1720:28	1082	82.86	40.85	0.641
650204	0417:53	956	84.80	41.47	0.157
650204	1603:0ɣ	1081	77.70	40.69	0.911
650204	1749:02	1080	85.94	42.45	0.721
650205	0301:11	948	78.51	40.30	0.306
650205	1445:56	1080	72.46	41.21	0.925
650205	1631:02	1079	79.98	41.17	0.684
650206	0143:32	945	72.92	40.69	0.196
650206	0327:50	948	81.46	41.14	0.106
650206	1513:26	1079	75.37	41.03	1.113
650206	1658:09	1078	82.91	41.14	0.768
650207	1540:50	1076	77.76	40.96	0.886
650208	1423:22	1075	72.61	41.22	0.785
650208	1608:13	1075	80.18	41.03	1.025
650209	1450:53	1073	75.49	41.10	1.027
650209	1635:14	1074	83.26	40.90	0.834
650210	0148:05	932	76.17	40.63	0.199
650210	1518:24	1070	77.81	41.13	0.997
650211	1400:24	1069	72.80	40.88	0.981
650211	1545:34	1068	80.34	41.01	0.847
650212	0057:40	927	73.42	41.13	0.197
650212	0242:41	926	81.84	40.88	0.125
650212	1428:15	1066	75.62	41.10	0.801
650212	1612:42	1067	83.43	41.01	0.792
650113	1455:40	1063	78.02	41.05	0.975
650214	0151:59	923	79.18	41.37	0.102
650214	1337:48	1062	72.95	40.89	1.088
650214	1522:5ʰ	1061	80.51	41.02	0.867
650214	0035:02	917	73.52	41.02	0.205
650215	0220:11	916	82.03	40.63	0.154
650215	1405:25	1059	75.78	40.91	0.935
650215	1550:13	1058	83.60	41.17	0.891
650216	1432:47	1056	78.22	40.83	0.847
650217	0129:51	912	79.23	40.78	0.142
650217	1315:27	1053	73.07	41.17	0.853
650217	1500:06	1063	80.74	40.86	0.870
650218	0012:22	910	73.64	40.95	0.154
650218	0157:11	909	82.27	40.95	0.159

DATE	TIME	HEIGHT	LONG	LAT	$\int Ndh$
650218	1342:47	1050	75.91	40.92	1.100
650219	0039:21	909	76.76	41.19	0.151
650219	1410:11	1046	78.34	40.08	1.052
650220	0106:52	906	79.43	41.04	0.163
650220	1252:46	1043	73.21	41.12	1.083
650220	1437:47	1042	80.80	41.17	0.944
650220	2349:06	905	74.04	41.52	0.124
650221	0134:24	903	82.49	41.03	0.142
650221	1320:02	1040	76.05	40.82	0.994
650221	1604:54	1039	84.11	41.20	0.712
650222	0017:16	900	76.70	40.51	0.098
650222	1347:41	1034	78.43	41.02	0.764
650223	1229:58	1032	73.36	40.97	1.225
650223	1414:57	1031	81.04	41.03	1.328
650224	0109:58	903	83.08	43.10	0.131
650224	0257:34	1027	76.13	41.00	0.950
650224	1442:05	1028	84.49	41.07	0.991
650225	1324:49	1024	78.62	40.85	0.875
650227	1234:47	1015	76.28	40.88	0.969
650227	2331:31	894	77.07	40.78	0.158
650228	1116:57	1014	69.88	40.92	0.788
650228	1302:09	1012	78.76	40.86	0.999
650311	1144:46	1008	73.60	41.08	1.095
650301	1329:26	1008	81.50	40.88	1.205
650301	2241:41	893	74.15	40.58	0.218
650302	1212:09	1003	76.40	40.92	1.088
650302	1356:44	1004	85.10	41.10	1.231
650303	2335.50	893	80.07	41.14	0.347
650304	1122:06	995	73.72	41.09	0.960
650304	1306:52	996	81.65	41.02	0.883
650304	2218:44	893	74.41	40.80	0.237
650305	1149:36	991	76.49	40.99	1.077
650306	1217:01	986	79.00	41.09	1.005
650307	1059:15	984	73.86	40.91	1.139
650307	1244:02	984	81.92	40.89	1.113
650307	2155:54	894	74.61	40.88	0.210
650307	2340.34	895	83.52	41.22	0.141
650308	1126:59	977	76.60	41.13	0.964
650308	2222:37	896	77.67	41.47	0.201
650309	1009:08	975	70.31	41.15	1.035
650309	1154:11	974	78.72	40.95	1.256
650309	2106:35	898	70.63	40.16	0.312
650310	1036:38	971	73.97	40.98	0.907
650310	1221:31	970	82.06	41.09	0.983
650310	2133:06	898	74.81	70.94	0.264
650311	1104:04	966	76.77	40.92	0.742
650311	1248:29	968	86.24	40.96	0.941

DATE	TIME	HEIGHT	LONG	LAT	$\int Ndh$
650311	2200:38	900	77.61	40.66	0.231
650312	1132:32	961	79.33	41.01	0.826
650312	2043:03	901	71.44	41.11	0.360
650312	2227:28	900	80.54	41.29	0.241
650313	1013:53	959	74.10	40.94	0.901
650313	1158:42	959	83.34	40.98	1.230
650313	2110:34	903	74.90	40.69	0.357
650314	1041:14	955	76.92	40.80	0.965
650314	2137:23	905	77.94	41.19	0.401
650315	0923:31	952	70.62	40.86	0.775
650315	1108:46	950	79.50	40.97	0.785
650316	1135:49	948	82.65	40.82	0.873

Acknowledgments

I wish to express my thanks to Dr. William J. Ross for his suggestion of this problem and his guidance throughout the course of the work. The assistance of the technicians and computresses of the Ionosphere Research Laboratory is acknowledged.

Appreciation is expressed to the Goddard Space Flight Center for providing both the orbital ephemeris and the tabulations of magnetic field components.

Support for this work came from the National Aeronautics and Space Administration under Grant NsG-114-61.